To Synthesize and Study Electrical Properties of Strontium Hexaferrites Doped with Magnesium, Cobalt and Lithium

By

Hina Waris

School of Chemical and Materials Engineering

National University of Sciences and Technology

2021

To Synthesize and Study Electrical Properties of Strontium Hexaferrites Doped with Magnesium, Cobalt and Lithium

Name: Hina Waris

Reg no: 00000274027

This thesis is submitted as a partial fulfillment of the requirements for the degree of

MS in (Nanoscience and Engineering)

Supervisor Name: Dr. Usman Liaqat

School of Chemical and Materials Engineering (SCME)

National University of Sciences and Technology (NUST)

H-12, Islamabad, Pakistan

June, 2021

Dedication

I dedicate this thesis to my family, the symbol of love and giving, my father Muhammad Waris, my mother Jamal Fatima and my siblings, my friends, my colleagues and my supervisor Dr Usman Liaqat and Co-supervisor Dr Iftikhar Husaain Gul, who has been a constant source of knowledge and inspiration, I could not be able to achieve this milestone without them. My this work is a symbol of love and appreciation for them.

Acknowledgements

Praise is to the almighty, the great and merciful Allah, who is supply of all expertise and wisdom, taught us what we knew not. We provide our humblest thanks to the Holy Prophet who is all time a version of steerage and expertise for humanity.

I am thankful to my affectionate superviser Dr.Usman and Co-supervisor Dr.Iftikhar Hussain Gul for their inspiring guidance, top notch suggestions,constructive criticism and co-operation for the duration of our project work. Without their aid and guidance, this work could not have been possible.

I am highly indebted and have no words to thank my friends for continuous support, generosity, effort and guidance, without them it is totally impossible to reach this stage.

I am highly grateful to my parents, and all the family members, for their prayers, unconditional love, continuous support and efforts through out my life.

My heartfelt thanks to all my colleagues for giving me encouragement, appreciation and help in completing this project.

Sincerely,

Hina Waris

Abstract

There has been a tremendous interest in hexagonal ferrites during the last ten years for a number of marvelous applications. “Due to their expended use”, hexaferrites has become very important magnetic material being commercially produced. Strontium based M type hexaferrites, $SrFe_{12}O_{19}$ is one of such material that is currently used in these applications. In the current work cobalt, magnesium and lithium dopant substitution is performed in series of $SrFe_{(12-3x)}(Co,Mg,Li)_xO_{19}$ (x=0.0,0.15,0.25,0.50) using sol gel method. The aqueous solution, containing metal nitrates were brought in use to prepare strontium hexaferrites nanoparticles. The prepared samples were then calcined at 950 ^{0}C for 4 hours. The synthesized samples were then characterized using X-ray diffraction (XRD), Scanning Electron Microscope (SEM) and Fourier Transform Infra-Red Spectroscopy (FTIR). Impedance analyzer and LCR meter was used for performing dielectric measurements. The formation of hexagonal $SrFe_{(12-3x)}(Co,Mg,Li)_xO_{19}$ was confirmed using XRD. Debye Scherer equation was used to find out the crystallite size that was in range of 37 nm-57 nm. The band positions were studied using FTIR. The study of dielectric properties with change in frequency was done at room temperature. For the cobalt, magnesium and lithium doped strontium hexaferrite nanoparticles the real part of dielectric constant enhanced to 77.8 at 250 Hz for x=0.5. the value of dielectric loss for cobalt, magnesium and lithium doped strontium hexaferrite nanoparticles has increased from 2.21 to 54.0 at 250 Hz. Ac conductivity values also showed increase in cobalt, magnesium and lithium doped strontium hexaferrite. AC conductivity results explains that electron hopping governs the conduction process. The electrical properties and conductivity rises with increasing concentration of cobalt, magnesium and lithium. The enhanced dielectric properties and increase in conductivity of the prepared nanoparticles make it applicable in field of super capacitors and charge storage devices.

Table of Contents

1 Introduction.....1
1.1 History of Ferrites 1
1.2 Paramagnetic Materials 1
1.3 Diamagnetic Materials 2
1.4 Ferromagnetism and Ferrimagnetism.....3
1.5 Super-Para Magnetism 3
1.6 Anti-Ferromagnetism 4
1.7 Classification and Types of Ferrites.....4
1.7.1 Spinel Ferrite.....4
1.7.2 Garnet.....5
1.7.3 Ortho Ferrites 5
1.7.4 Hexagonal Ferrites 5
1.8 Ferrites.....6
1.8.1 Hard Ferrites.....6
1.8.2 Soft Ferrites.....6
1.9 Hexagonal Ferrites 7
1.9.1 Structure of M- Type Hexaferrites.....8
1.9.2 Classification.....8
1.9.3 Structure of M-Type Strontium Hexaferrites.....8
1.10 Properties of Hexagonal Ferrite 9
1.10.1 Magnetic Properties of Hexagonal Ferrites.....9
1.10.2 Electrical Conductivity of Ferrites:.....9
1.10.3 Dielectric Properties.....9
1.11 Methods of Synthesis of Hexagonal Ferrites 10
1.11.1 Sol-Gel Method.....10
1.12 Significance of Ferrites 11
1.13 Application of Ferrites.....11
1.14 Objectives.....12
2 Theoretical review.....13
2.1 Synthesis of Nanoparticles 13
2.1.1 Top Down Approach.....13
2.1.2 Bottom Up Approach 13
2.2 Literature Study.....15
2.3 Sol-Gel Method 20
2.4 Experimental Details 20
2.4.1 Materials.....20
2.5 Synthesis of Strontium Hexaferrites.....21
2.5.1 Synthesis of $SrFe_{12}O_{19}$ with Co, Mg and Li Dopant.....21
2.6 Sample Preparation.....23
2.6.1 Preparation of SEM Samples: 23
2.6.2 Preparation of FTIR Samples.....23
2.6.3 Preparation of Samples for Measurement of Electrical Properties 23
3 Introduction to Sample Characterization Techniques.....24
3.1 X-Ray Diffraction Technique.....24
3.2 Basic Principle for XRD.....25

3.3 Lattice Constant....26
3.4 Crystallite Size....27
3.5 X-Ray Density....27
3.6 Scanning Electron Microscopy....28
3.6.1 Basic Principle of SEM....28
3.7 Fourier Transform Infra-Red Spectroscopy....29
3.7.1 Working Principle of FTIR....29
3.7.2 Applications of FTIR....30
3.8 Electrical Properties....30
3.8.1 Dielectric Properties....31
3.8.2 AC Impedance Spectroscopy....32
3.8.3 Electric Modulus....32
3.8.4 Two probe method....32
4 Results and Discussions....35
4.1 X-Ray Diffraction Results....35
4.2 Scanning Electron Microscopy Results....37
4.3 Fourier Transform Infra-Red Spectroscopy Results....38
4.4 Dielectric Studies....40
4.4.1 Dielectric Constant....41
4.4.2 Dielectric Loss....42
4.4.3 Variation of AC Conductivity....46
4.4.4 Impedance....48
Conclusions....50
Future Work....52
References....53

List of Figures

Chapter 1 - Introduction

1.1 Configuration of atomic diploes for paramagnetic materials 2

1.2 Atomic dipole ordering for diamagnetic materials 2

1.3 Ordering of dipoles for ferromagnetic and ferromagnetic materials 3

1.4 Atomic dipole configuration for super-paramagnetic materials 3

1.5 Ordering of dipoles for anti-ferromagnetism 4

1.6 Stacking of hexagonal closed packed-lattice 7

1.7 Crystallographic structure of strontium hexaferrite 9

Chapter 2 - Literature Review

2.1 Step-by-Step Sol gel process 22

2.2 Pellets of ferrites 23

Chapter 3 - Introduction to Sample Characterization Technique

3.1 Incident x ray beam scattered by atomic plane in a crystal 25

3.2 Diffracted cones of radiations forming in powder method 26

3.3 Schematic figure of scanning electron microscope 28

3.4 Schematic figure of FTIR spectroscopy 29

3.5 Schematic figure of impedance analyzer 30

3.6 Schematic figure of two probe method 32

Chapter 4 - Results and Discussion

4.1 XRD pattern of pure strontium hexaferrite 34

4.2 XRD pattern of Co, Mg and Li doped strontium hexaferrite 35

4.3 SEM image of pure strontium hexaferrite 36

4.4 SEM image of $SrFe_{(12-3x)}(Co,Mg,Li)_xO_{19}$ for x=0.15 37

4.5 SEM image of $SrFe_{(12-3x)}(Co,Mg,Li)_xO_{19}$ for x=0.25 37

4.6 SEM image of $SrFe_{(12-3x)}(Co,Mg,Li)_xO_{19}$ for x=0.5 37

4.7 FTIR spectra of pure strontium hexaferrite 38

4.8 FTIR spectra of Co, Mg, Li doped strontium hexaferrite 39

4.9 Dielectric constant variation with the frequency for $SrFe_{(12-3x)}(Co,Mg,Li)_xO_{19}$ 41

4.10 Dielectric constant variation at 250 Hz for $SrFe_{(12-3x)}(Co,Mg,Li)_xO_{19}$ 41

4.11 Dielectric loss variation with the frequency for $SrFe_{(12-3x)}(Co,Mg,Li)_xO_{19}$ 43

4.12 Dielectric loss variation at 250 Hz for $SrFe_{(12-3x)}(Co,Mg,Li)_xO_{19}$ 43

4.13 Dielectric tangent loss variation with the frequency for $SrFe_{(12-3x)}(Co,Mg,Li)_xO_{19}$ 45

4.14 Dielectric tangent loss variation at 250 Hz for $SrFe_{(12-3x)}(Co,Mg,Li)_xO_{19}$ 45

4.15 AC conductivity variation with the frequency for $SrFe_{(12-3x)}(Co,Mg,Li)_xO_{19}$ 47

4.16 AC conductivity variation at 250 Hz for $SrFe_{(12-3x)}(Co,Mg,Li)_xO_{19}$ 47

4.17 Impedance real part Z’ variation with the frequency for $SrFe_{(12-3x)}(Co,Mg,Li)_xO_{19}$ 49

4.18 Impedance imaginary Z” part variation with the frequency for $SrFe_{(12-3x)}(Co,Mg,Li)_xO_{19}$ 49

List of Tables

1.1 Metallic Sub-Lattices of M Type Hexaferrites 8

List of Abbreviations / Acronyms

No	Abbreviation / Acronym	Meaning
1	**Sr**	Strontium
2	**NPs**	Nanoparticles
3	**NCs**	Nanocomposites
4	**XRD**	X-ray diffraction Technique
5	**SEM**	Scanning Electron Microscope Technique
6	**UV-Vis Spectroscopy**	Ultra-Violet Spectroscopy
7	**FTIR**	Fourier Transform Infra-red Spectroscopy
8	**DC**	Direct Current
9	**AC**	Alternating Current

Chapter 1

Introduction

1.1 History of Ferrites

The history of ferrites and their applications have been known for several centuries ago. Naturally occurring magnetite is vulnerably tough. Hard ferrites own magnetism which is basically permanent. Basically the ferrites are ceramic substances, which are dark grey or black in the appearance and are very hard and brittle. Spinal ferrites have been widely used in electronics applications for last century[1]. It is considered as the most useful ferromagnetic material. They consists of both hard and soft ferrites as they have been in applications for past many years. Nano ferrites are synthesized via numerous techniques Normally these techniques which are used can be divided in the two classes which is wet chemical method and solid state method. Usually the wet chemical method is desired as this offers homogeneous nanoparticles also the annealing temperature is likewise low that gives small size annoparticles [1].

1.2 Paramagnetic Materials

Materials with paramagnetic behaviour posses permanent magnetic dipole moments due to the incomplete cancellation of the electron spins and the orbital magnetic moments. In the absence of an applied field, dipole moments are randomly oriented therefore a material has a no net macroscopic magnetization. In the absence of magnetic field ferro and ferri magnets have permanent magnetic moments and large permanent magnetization. In ferromagnetic materials, this permanent magnetic material is a result of combined interaction of large number of atomic spins that are known as domains, these are regions where alignment of the spins is in the same direction. The external magnetic field then causes the electron spins to align themselves parallel to field to cause a net attraction [2].

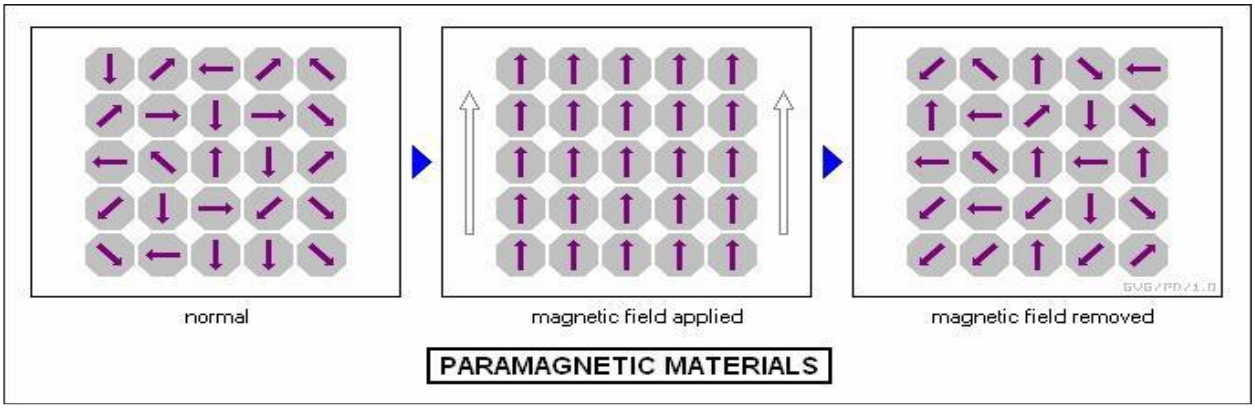

Fig 1.1 Configuration of atomic dipoles for paramagnetic material [2]

1.3 Diamagnetic Materials

These materials which are when placed in the magnetic field, then becomes weakly magnetized in the direction which is opposite to that of applied field. Electrons move around an atom in orbitals and when magnetic field is applied, this orbital motion of electron give rise to diamagnetism. This orbital motion is responsible for the generation of magnetic field which opposes the applied magnetic field. Therefore, the net magnetic moment of an atom is zero in case of diamagnetic materials. As soon as the magnetic field is removed, magnetization in these materials again drops down to zero because thermal intrinsic energy is higher than the potential energy which aligns the dipole and dipole moments tend to randomize due to thermal agitation [3].

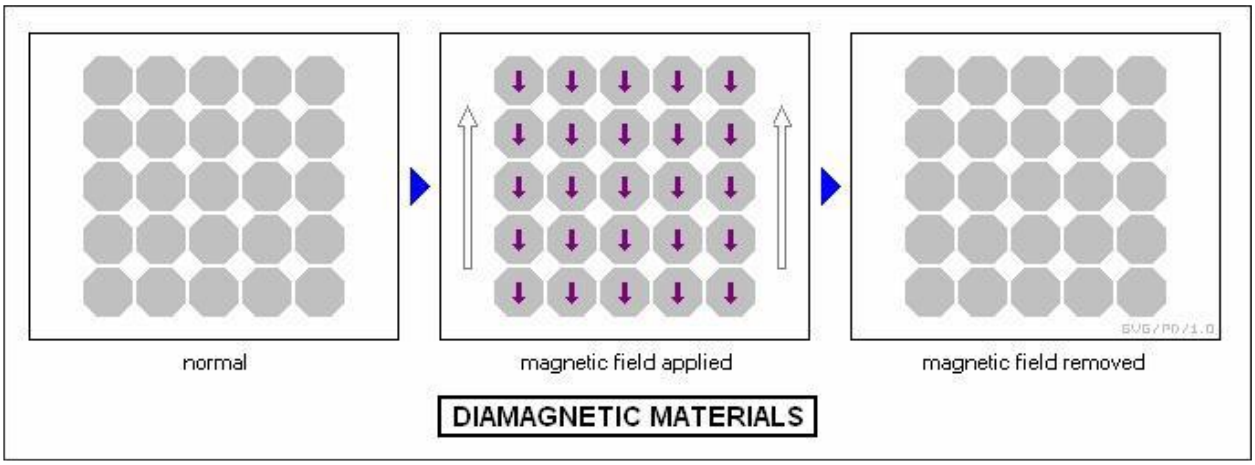

Fig 1.2 atomic dipole ordering for diamagnetic material [3]

1.4 Ferromagnetism and Ferrimagnetism

The material which possess permanent magnetization which is not in presence of the external magnetic field is known as ferromagnetic and ferromagnetic materials. Permanent magnetization values are large in these materials. Atomic spins also known as domains, interact with each other in such a way which results in the alignment of all spins in the same direction.

The permanent magnetization observed in the case of ferromagnetic material is due to incomplete magnetic field cancellation. This will result in magnetization which is permanent but of low magnitude. If all the dipoles present in the sample will get aligned than their sum will result in macroscopic magnetization in ferromagnetic and ferrimagnetism materials. Ionic solids are electrically insulating so is ferromagnetic materials. Ferromagnetic materials are mostly metals [4].

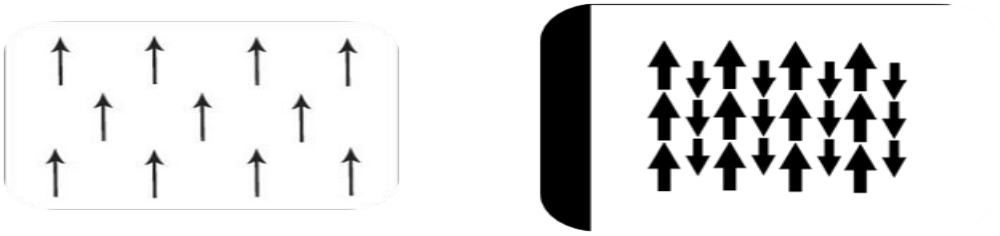

Fig 1.3 ordering of dipoles for ferromagnetic and ferrimagnetic materials [4]

1.5 Super-Para Magnetism

The super-paramagnetism arises when a material is subjected to temperature less than curie temperature. This will result in the alignment of neighboring atom's magnetic moments [5].

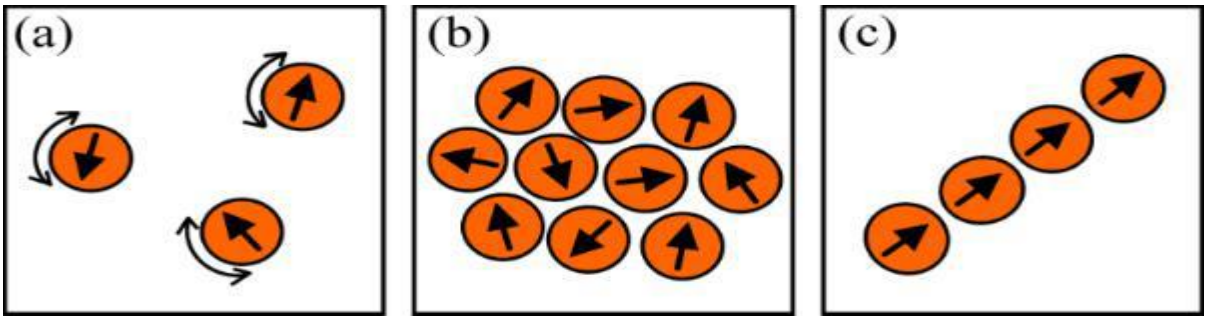

`Fig 1.4 atomic dipoles configuration of super-para magnetic materials [5]

1.6 Anti-Ferromagnetism

The magnetic moments or electron spins aligned in regular pattern to the spins of neighboring atoms but oriented in opposite direction will result in anti-ferromagnetism. This specific kind of behavior is observed at very low temperature and it vanishes above a fixed temperature. This temperature is known as Neel temperature [5].

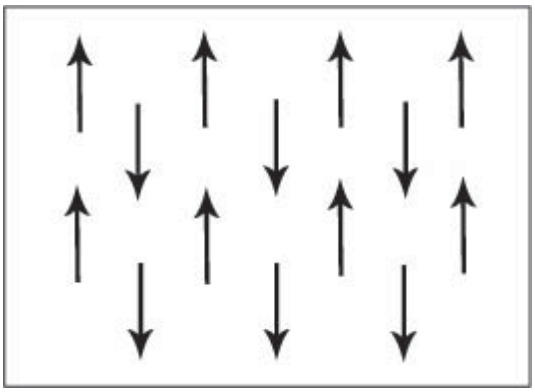

Fig 1.5 Order of dipoles for Antiferromagnetsim [5]

1.7 Classification and Types of Ferrites

Ferrites are made up of iron oxides as their essential constituent element and metal oxides. Depending on crystal structure, ferrites consists of following types.

- Spinel ferrites.
- Garnet ferrites.
- Ortho ferrites.
- Hexagonal ferrites.

1.7.1 Spinel Ferrite

AB_2O_4 represents the crystal structure of spinel ferrite where A and B represents divalent and trivalent cations respectively. Examples of divalent cation include Co^{2+} Ni^{2+} Zn^{+2} Mn^{+2}, Mg^{+2} and trivalent cation can be iron or aluminum etc. Crystal structure of spinel ferrite is acquired from $MgAl_2O_4$, a mineral spinel. Unit cell structure of these spinel ferrites is cubical, and each unit cell contains eight smaller unit cells which are called octanes or formula units. Each unit cell is comprising of 32 oxygen atoms, forming a lattice which is face centered cubic in structure with tetrahedral and octahedral sites. Tetrahedral sites are denoted by A sites and they are

surrounded by four oxygen atoms while six oxygen atoms surround the octahedral sites, represented as B sites. The spinel ferrite structure is not electrically neutral because when metal ions of valency of either +2 or +3 are filled in A and B sites, positive charge dominates [6].

1.7.2 Garnet

Garnets are the second group of ferrites with general formula $Me_3B_5O_{12}$ where A represents a rare earth metal cation like yttrium where B represents iron. The unit cell of garnet ferrites is cubical, and it contains eight smaller formula units. In garnet ferrites are comprised of; Tetrahedral A sites, Octahedral B sites and Dodecahedral C sites. A and B sites have distribution of iron cations (Fe^{3+}) in the ratio of 3:2 while dodecahedral C sites are occupied by Me cations, surrounded by the oxygen atoms. Garnet is known for their optical transparency and for their magneto-optical applications [6].

1.7.3 Ortho Ferrites

Ortho ferrites are third group of ferrites with distorted perovskite structure having a general formula of ABX3 where A is a rare earth or alkaline metal cation, B belongs to transition metal cation usually Iron and X is anionic specie, which is oxygen, in most cases. In orthoferrites, an octahedra is formed by Fe, being the central ion and coordinated by six oxygen atoms. The interstitial sites in octahedral structure are filled by the A cations coordinated by 12 oxygen atoms. Ortho ferrites are known for their high domain wall velocities and have applications in magnetic field sensors, communication technique and electronic current etc [6].

1.7.4 Hexagonal Ferrites

Hexaferrites were first discovered in 1950's and developed over past several decades. Hexaferrites based on barium, strontium and calcium along with iron possess high coercivity and permeability values and can conduct magnetic flux well. This polycrystalline ferrite gained considerable attention in electronic industry because of low cost, easy manufacturing and remarkable electric and magnetic properties.

Hexa-ferrites belong to fourth group of ferrites having hexagonal structure and they are further divided in to six classes named as: M, U, W, X, Y and Z. A large number

of hexaferrites can be prepared using different compositions with contrasting magnetic properties [6].

1.8 Ferrites

A ferrite is a ceramic material synthesized by the mixing and the firing of the large quantity and proportions of iron (111) oxide, which is then blended in small portions of one or more than one additional metallic elements such as barium, manganese, nickel and zinc. These are electrically not conductive i.e. they are the insulators also the term ferrimagnetism means that they can easily get magnetized or attracted to a magnet. Ferrites are divided into the two families based on their resistance to get demagnetized [7]. `

1.8.1 Hard Ferrites

Hard ferrites have high coerctivity so they are relatively difficult to get demagnetize. They are used to synthesize permanent magnets for the applications such as refrigerator magnets, loud speakers, and small electric motors. Due to low price of raw material, hard ferrite magnets are most inexpensive type available. Hard ferrite magnets have relatively good electrical isolation effects and are difficult to demagnetize even in strong external magnetic fields. Their corrosion tendency is low, which makes them very suitable for liquid applications. Disadvantage are that they are easily breakable and have low tensile strength. The strength and brittleness of the hard ferrites are just like ceramics, moreover the temperature resistance is restricted and they have a low energy to volume ratio [7].

1.8.2 Soft Ferrites

This material includes a high electrical resistance and excellent magnetic characteristics in the range of high frequency although the saturation flux density is slightly lower than the other soft magnetic materials. They are called as non-permanent magnets; they maintain magnetism but as soon as the magnetic field is being removed, the magnetism vanishes. Soft ferrites are known for their popularity as transformers (to change the voltage from primary to secondary windings) hence soft ferrites are often called as the transformer ferrites. Soft ferrites exist in different shapes such as toroids (rings), c shapes, e shapes, curved shapes, etc. other shapes are

also possible. They often have their criteria for performance such as permeability and inductance [7].

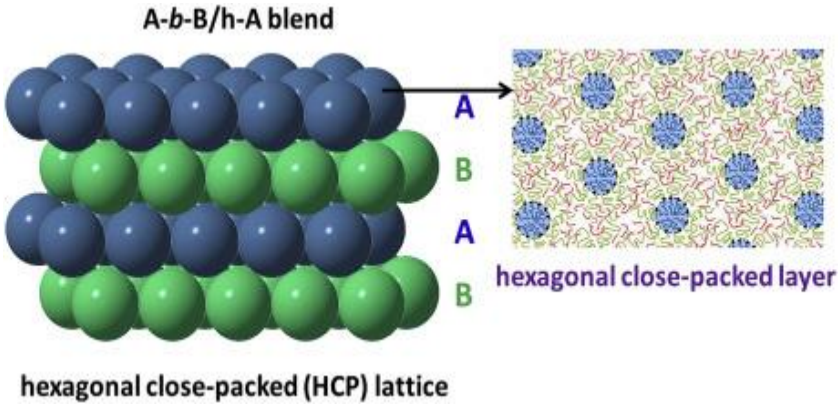

Fig 1.6 stacking of hexagonal closed packed lattice [7]

1.9 Hexagonal Ferrites

Hexaferrites obey the formula $MO+MeO/Fe_2O_3$ where M corresponds to the metals like barium, strontium, calcium etc. whereas Me represents transition metal cation like iron, cobalt, manganese etc. There is a close packing of Oxygen ions layer in the crystal structure of hexaferrite and any divalent of trivalent metal cation reside in the interstices of the structure. Substitution of heavy metal ions like Ba or Sr occur in the oxygen layers. In hexaferrites, there are essentially 3 fundamental structural blocks names as: S, R and T and they have a rotational symmetry at 180^o around the hexagonal c axis represented as S*, R* and T* respectively.

A neutral (RS) block with the total composition of $MFe_{12}O_{19}$ (M Phase) is formed when R subunit combines with S^{+2}. Similarly, a neutral TS can be formed when T subunit combines with S0 with total composition of $Ba_2Me_2Fe_{12}O_{22}$, called as Y phase. Likewise, different composition like X, Y, Z, W, and U can be formed by varying the stacking sequences of hexagonal and cubic units These sub lattices, their coordination number and the number of metal ions in each, are listed in the table below [8]

Block	Sub Lattice	Coordination	Ions per unit Cell	Spin Direction
	$4f_1$	Tetrahedral	4	Down
	2*a*	Octahedral	2	Up
R	$4f_2$	Octahedral	4	Down
	2*b*	Bi-pyramidal	2	Up
S-R	12*k*	Octahedral	12	Up

Table 1: The metallic sub-lattices of M-type hexaferrite [8]

1.9.1 Structure of M- Type Hexaferrites

Ferrites with hexagonal structure are called hexagonal ferrites, hexagonal ferrites are divided into six different types M, W, Y, X, U and Z. a ferrite having high value of coercivity Hc is known as hard ferrite and having low value of coercivity Hc is called soft ferrite [9].

1.9.2 Classification

Hexagonal ferrites are divided into six different types according to chemical composition and crystal structure M (AFe12O19), W (AMe2Fe16O27), X (A2Me2Fe28O46), Y (A2Me2Fe12O22), Z(A3Me2Fe24O41), U(A4Me2Fe36O60); where A = Ba2+, Sr2+, La2+, Pb2+ and Me = a bivalent transition metal. These ferrites have extensive magneto crystalline anisotropy and possess magnetoplumbine structure. The compounds BaFe12O19 (BaM), SrFe12O19 (SrM) and PbFe12O19 (PbM) are M type hexagonal ferrites [10]

1.9.3 Structure of M-Type Strontium Hexaferrites

The composition of fundamental structural R and S blocks in SrM is $SrFe_6O_{11}$ and Fe_6O_8 respectively. R and S blocks are stacked in M Type Strontium hexaferrite to form a unit cell in sequence RSR*S* where the sign star denotes the 180^o rotation about the c-axis of the hexagonal lattice. Therefore, two $SrFe_6O_{11}$ molecules are present in the unit cell of SrM. Four oxygen ions are present in each of the two hexagonal layers in S Block while R block constitutes three hexagonal layers of oxygen. One oxygen ion in the middle hexagonal layer in R block is replaced by a strontium ion. Five interstitial sites are occupied by the metal ions in the unit cell of SrM.

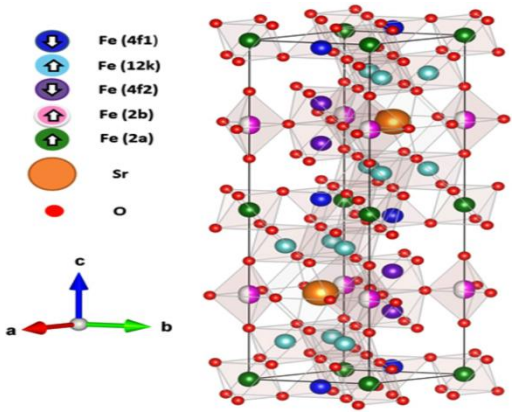

Fig 1.7 Crystallographic structure of $SrFe_{12}O_{19}$ [10]

1.10 Properties of Hexagonal Ferrite

1.10.1 Magnetic Properties of Hexagonal Ferrites

In large metal ions like barium and strontium, the size of crystal lattice is varied. This forms the basis of magneto-crystalline anisotropy which results in distinct magnetic properties in hexaferrites. The magnetization in most of the hexagonal ferrites is shown in the direction of c-axis because of which their XRD pattern dif3fer from any other ferrites oriented in random order. Magnetic properties of hexagonal ferrites can be altered by the addition of metal cations by doping. With the addition of metal cation like aluminum, gallium or chromium, the magnetic anisotropy and magnetization of barium hexaferrite can be enhances [10].

1.10.2 Electrical Conductivity of Ferrites:

Owing to distinct electrical properties of ferrites, they are applicable for various electronic applications. The conduction mechanism in ferrites differ from semiconductors as in ferrites the temperature affects the charge carrier mobility in turn effecting the conduction mechanism. Charge carriers in ferrites are localized at the magnetic atoms and carrier concentration in independent of temperature. Hopping of 3d electrons between Fe^{+2} and Fe^{+3} causes the conduction in ferrites. Closely packed oxygen anions surround the metal cations causing the isolation of electron to a particular ion and there is a small overlapping of anionic cloud or orbital. Due to isolation of each electron to a particular ion, localized electron model is more significant in ferrites as compared to band model [11].

1.10.3 Dielectric Properties

Dielectric properties mainly include dielectric constant, loss, tangent loss and ac conductivity, impedance and electric modulus. The information about the formulation

of electric field in the material can be gained from these properties. In ferrites, electric hopping between Fe^{+2} and Fe^{+3} shows the prominent conduction mechanism [12].

1.11 Methods of Synthesis of Hexagonal Ferrites

The formation of hexaferrites is an extremely complicated process and the mechanism involved is not fully understood despite having been investigated by many researchers for over 50 years. For synthesizing nanoparticles, there are various methods and each one has some advantages and disadvantages too. The various methods of synthesis possess different magnetic, structural and electrical properties. The various methods are

- Standard Ceramic Technique.
- Co-precipitation.
- Salt-metal method.
- Hydrothermal process.
- Sol-gel method.

We will discuss sol-gel method in detail as we have used this method for the preparation of the Samples [13].

1.11.1 Sol-Gel Method

The sol gel method is considered effective to modify the surface of substrates. Obtaining of a high surface area and stable surfaces is the most important advantage of the sol gel method. The chemical and physical properties of the materials obtained by the sol gel method are related to the experimental conditions applied. The sol gel method involves two main reactions.

1) Hydrolysis of the precursor in the acidic or basic medium.

2) Polycondensation of the hydrolyzed products.

In this way a polymeric network is formed in which MNPs can be retained.

Sol gel process provides a new approach to the preparation of new materials. This process allows a better control of the whole reactions involved during the synthesis of solids. homogeneous multi component systems can be easily obtained, particularly homogeneous mixed oxides can be prepared by mixing the molecular precursor solution. The chemistry of the sol gel process is based on hydrolysis and polycondensation reactions. Sol gel method is useful for applications of functional

materials such as photo catalyst, nonlinear optical materials, ferroelectrics and superconductors. For this purpose, sol gel preparation of simple and complex non silica oxides, including TiO_2, ZrO_2, Al_2O_3, rare earth oxides and so on have to be studied. Metal lakesides are often employed for those oxides. Most of them are however, are unstable, that is, they are rapidly hydrolyzed and are easily precipitated which makes it difficult to form homogeneous multicomponent oxide products [14].

1.12 Significance of Ferrites

The magnetic materials like iron and its alloys are used in various technologies. The reason for their use is their low Dc resistivity. But some applications like electrical circuits and cores of inductors cannot make use of iron and its alloys as these are applications requiring high frequencies. The current that induce in the circuit start flowing in the material. This problem is heat generation due to presence of low electrical resistivity. This will result in the release of energy in atmosphere posing serious issues. The energy losses make the material incompatible at high frequencies. The ferrites on the other hand, shoed better performance because of their high DC resistivity values. Some properties like relatively high permeability and stability with temperature have also opened way for its use in applications involving high frequencies like electronic circuits, adjustable inductors, filter circuits and delay lines etc. The ferrite applications for high frequencies are more usual. Another reason for their use is they are relatively less expensive as compared to other alloys. In case of material requirement that has low volume, high quality, low cost, and high stability ferrites are considered to be best for frequency ranges of 10 KHz to MHz also ferrites offer flexible mechanical and magnetic parameter that none of other metal has offered [15].

1.13 Application of Ferrites

For the excellent performance in the application and classified by the initial permeability for the low and high frequency applications, the most essential technological properties are saturation magnetization(Ms), coercive force(Hc), initial permeability(ui) and losses [16]. The other applications of ferrites are given as under:

- High density write once for optical recording.
- Magnetic shielding.
- Pollution control.

- Ferrite electrodes.
- Entertainment ferrites.
- Power transformers and chokes.
- Inductors and tuned transformers.
- Pulse and wide band transformers.
- Magnetic deflection structures.
- Recording heads.
- Rotating transformers.
- Shield beads and chokes.
- Transducers.
- Catalysis.
- Optical properties.
- Light scattering.
- Drug delivery.
- Pesticide delivery.
- Magnetic recording.

1.14 Objectives

This research work has following objectives:

- To use a very easy and cheap sol-gel method for the fabrication of $SrFe_{12}O_{19}$ nanoparticles which have the hexagonal structure.
- To get the information on the effect of Co, Li and Mg on dielectric properties.
- Effect of the doping on the electrical properties at different concentrations of Co, Mg and Li.

Chapter 2

Theoretical review

2.1 Synthesis of Nanoparticles

Nanoparticles can be fabricated by following ways given below:

- Top down approach.
- Bottom up approach.

2.1.1 Top Down Approach

The process of cutting of the bulk material is involved in this approach to get Nano size particle. A large amount of useful nanostructures is fabricated by using various top down fabrication techniques. Some of these techniques are molding, lithography, embossing and skiving.in lithography electron or light beam is made to fall on a selective portion of device. A variety of elements in semiconductor industry is made using lithography. For instance, integrated circuits, masks etc. ceramic industry also employ top down method for making alloys. Top down method has variety of applications on commercial level. Also there are some drawbacks associated with top down method

- A significant amount of impurity is present in the products synthesized using this method.
- The structure established initially might have to be changed in roll out phase [17].

2.1.2 Bottom Up Approach

In bottom up approach atoms and molecules combine together to form complex and stable structures. This is most widely used technique for synthesis of nanoparticles. Bottom up technique includes CVD, MBE, physical vapor deposition, electrochemical depositions, sol gel and co precipitation methods. It offers various advantages. It offers various advantages i.e. it is better, cheaper easy to handle and efficient. Nanoparticles can be synthesized by various methods. Every method poses a separate advantages and disadvantages. The chemical, structure and magnetic properties of prepared nanoparticles are dependent greatly on the method follow for synthesis [17]. Some of the synthesis methods are as follows:

- Sol gel method.
- Micro emulsion method.
- Co-precipitation method.
- Solvothermal method.
- Hydrothermal method.
- Gas condensation method.
- Sono-chemical method.
- Combustion flame synthesis.

At room temperature ferrites exhibit unique behavior and are applicable to many devices due to their unique properties. Ferrites have low electrical and high DC electrical resistivity. Spinal ferrites are preferred due to chemical stability, excellent magnetic properties, simplified synthesis process, reasonable cost and mechanical hardness. Presently hexaferrites are applicable in antennas cores, computer components, memory devices, permanent magnets, satellite communication, magnetic sensors and actuators, microwave absorbing materials, gas sensors, cancer treatment and in magnetic resonance imaging. due to the electrochemical performance, binary metal oxides are extensively applicable in electrochemical applications like capacitors, fuel cells, Li-ion batteries, the solar cells. The electrochemical capacitors employ oxides of transition metals having a spinal crystal structure as they provide a strong crystalline architecture with diffusion pathways in three dimensions. Presently a variety of spinal and inverse spinal ferrites have been tested for electrochemical capacitors. electronics and catalysis have been extensively employed transition metal oxides because of their high catalytic activity, environmental accordance and easy separation [18].

After the year 2000, the magnitude of work related to synthesis and characterization of ferrite nanoparticles have gain popularity. The change in property of material at nanoscale was the main cause for this increased research work the main focus of many conferences was to develop processing equipment and development of characterization techniques for synthesis and characterization of hexaferrites. also the application of ferrite particle in optical applications, microwave applications, multilayer chips inductor and Nano ferrite composite were considered. Hexaferrites are 90 percent of total magnets manufactured worldwide every year, mostly they are

used in tiny motor like windscreen wiper motor and in number of sensor applications [19].

2.2 Literature Study

R Martinez Garcia et al. $SrFe_{12}O_{19}$ fine particles were combined by the sol-gel technique and warmth treatment was completed in oxygen controlled environment. $SrFe_{12}O_{19}$ were prepared at 250 ^{0}C. The impact of $SrCO_3$ phase that hinders the hexaferrite in air at lower temperature is observed. The IR spectroscopy and XRD was used to study samples.TEM was used to study morphology [20].

Neil J. Shirtcliff et al. Sol gel route was followed to obtain aluminum doped strontium and barium hexaferrites nanoparticles $BaAl_XFe_{(12-X)}O_{19}$ to complex the ions. Citrus acid was used in reaction. Smaller particle size was obtained using this method. Structure retention in barium ferrite was seen by substitution of half of iron for aluminium, while strontium aluminium ferrite can be obtained with aluminium content having total substitution of iron. All materials that were synthesized have particle size less than 1 mm. when moving from iron to aluminium ferrites materials shows changes in structure and morphology. Such materials might guarantee for imaging applications [21].

Sadhana et al. Microwave hydrothermal method was used to synthesize Cr doped Sr hexaferrites ($SrCrxFe_{12-x}O_{19}$). Sintering was done at 950 ^{0}C for 90 min in a single mode microwave furnace. Anisotropic change was seen in lattice parameters by increasing Cr^{3+} content while c decreased and an increased.280-660 nm average grain size was obtained. From XPS spectra presence of both Fe^{2+} and Fe^{3+} ions in structure of crystal is seen when Cr^{3+} is higher for x>0.3. Increased coercivity and decreased saturation magnetization by doping Cr^{3+} [22].

Prabhjyot Kaur et al. Nano crystalline particle of $SrZr_xCo_xFe_{(12-x)}O_{19}$ has been synthesized through sol-gel and sucrose is used as fuel. FTIR, SEM, XRD, TEM, EDS and TGA-DTA have been used for characterization.VSM and MS have been used for study of magnetic properties. Effect was seen of temperature during calcination on magnetic properties and morphology of samples was investigated in the range of 500-1100 ^{0}C. formation of single phase hexagonal ferrites at 9000c is seen through XRD

analysis. Using Scherer equation crystallite size calculated lies in the ranger of 21-33 nm. structure, electrical and magnetic properties have effect of Zr and Co substitution for Fe. The saturation magnetization increasing from 62.27 eu/g to 64.84 emu/g up to value of x=0.40 and then decreases for x=1.0 to 49.71emu/g. in the frequency range of 20 Hz-120 Hz dielectric constant, dielectric tangent loss and Ac conductivity for all compositions have been studied [23].

Muhammad Javed Iqbal et al. chemical co precipitation method was used to get Zr-Zn doped strontium hexaferrites nanoparticles. For magnetic recording media application, a suitable signal to noise ratio is obtained as crystallite sizes are small enough of 30-47 nm. Metal to semiconductor transition when temperature ranges from 388 to 408 K is seen by Zn-Zr doped samples through DC resistivity depending on temperature. Zr-Zn content enhancing increases drift mobility, dielectric loss, and dielectric constant where activation energy and DC resistivity decreases for hopping. By substituting Zr-Zn content of x less than or equal to 0.4 value of remenance increases from 55 to 59 kAm^{-1}, increased saturation magnetization from 71 to 92 kAm^{-1} and magnetic moment from 11.2 to 13.6 μB while coercivity decreased from 137-34 kAm^{-1}. According to these parameters the materials synthesized can be used in recording media as a potential application [24]

Amin Ur Rashid et al. citrate gel technique was used for the preparation of mixed phase composite $SrFe_{12}O_{19}/MgFe_2O_4/ZrO_2$ for magnetic hyperthermia XRD, SEM and vibrating sample magnetometer were used for structure and magnetic analysis. By increasing Mg and Zr content the increase in magnesium ferrite and zirconium oxide phase is confirmed through data obtained by XRD and SEM.at room temperature magnetization loops were measured that show variation in saturation magnetization, remenance and coercivity that depend on highly anisotropic phase of Sr-hexaferrite. Lowest coercivity and saturation magnetization were obtained from sample with high Mg and Zr content. Potential for use in magnetic hyperthermia was suggest after observing heating effect in selected samples at 214 kHz and magnetic field of 22 Oe [25].

H.S. Singhal et al. worked on ferrite nanoparticles due to their remarkable dielectric and electric properties. They worked on nickel ferrite and substituted nickel ferrite.

The magnetic, electric and physical properties of nickel showed a remarkable improve when it is substituted with aluminium. So it can be concluded that the properties can be enhanced by making composite of nickel with other material. The study is needed to know the exact amount of substitution and method of preparation. The effect of preparation technique should also be known [26].

Fouzia Altaf et al. sol gel technique was used to synthesize Co-substituted strontium hexaferrite $SrFe_{12-x}CoxO_{19}$.XRD was used to determine crystal structure that confirms hexagonal structure without any impurity in all samples. Unit cell volume-ray density, lattice parameters, crystallite size and porosity of samples were obtained from X-ray diffractometer. Fe sites were affected by the substitution of cobalt in samples. Electrical measurements at low temperature showed increase in resistivity by increasing temperature that represents semiconductor behavior of samples [27].

C M Fang et al. density functional theory was used to study magnetic and electronic behavior of strontium hexaferrite. Ferrite ions are full spin polarized Fe^{3+} by S=5/2 according to calculations. Iron ions exchange interactions influence electronic structure of ferrites. Ferrimagnetic is most stable ferrite from having Fe^{3+} ions at 4f site having antiparallel spin polarization to other Fe^{3+} ions. Strontium ferrite has been calculated to be semiconductor with dominating Fe 3d state at top of valence band and bottom of conduction band. For conductive charge carrier's strong anisotropy found. Results calculated are good according to experimental data [28].

Avinash.V et al. Strontium Y type hexaferrite was substituted with cobalt $Sr_2Ni_{2-x}Co_xFe_{12}O_{22}$ where (x=0.5) by sol-gel technique to study effects of properties of strontium Y-type hexaferrite.TGA, XRD, DTA, SEM and FTIR were used for structure, morphology and thermal study. High pure single phase $Sr_2Ni_{2-x}Co_xFe_{12}O_{22}$ was formed with synthesis temperature 950 ^{0}C and time 48 hours. Lattice parameters calculated are a=5.8979 A^0 and c=44.4527 °A. Ferrites prepared have hexagonal morphology was analyzed through SEM. In hexagonal structure there are standard frequencies of vibration bands shown by absorption of IR absorption study that confirms the hexagonal the hexagonal structure of these samples. TGAs performed that confirms strontium hexaferrite thermal stability. Exothermic peak at 600 ^{0}C in DTA gives confirmation of strontium ferrite phase formed, Curie temperature was 120

^{0}C from dielectric study. To determine seebeck coefficient thermos electric study up to 250 ^{0}C was to be carried out [29].

A.E. Paladino et al. studied microwave properties of fine grain nickel ferrite at high peak power levels. The process used for synthesis of fine grain nickel ferrite at high peak power levels. The process used for synthesis of ferrite nanoparticles was hot press was ball milling and composite is prepared using flame spraying**.** The studies find out that with decrease in grain size absorption is increased. The value of dielectric loss also shows a reduction. The dielectric losses offered by low field also reduces with composition. Cobalt is also substituted in higher threshold fields. The prepared fine grained ferrite which was also hot pressed has operated at 750 KW/750 W power level. But a nonlinear behavior was observed below peak power of 20Kw [30].

A.P. Singh et al. studied microwave properties of conducting magnetic nanocomposites. They suggested that the electromagnetic properties of a composite having multiple phases can be improved by various methods. These methods include introduction of magnetic filler in a reasonable amount. Other methods involve design of such a medium that contains conducting, magnetic and dielectric material mixture as filler. A lot of studies have done in this field but scientists are still unable to find a material that will produce no reflection and give competent absorption. This is a challenging task the only possible solution is the use of material which can also be seen as the future possibility. The next generation material will form the building blocks of shielding material will be multi-phase and lightweight materials having excellent shielding properties [31].

Roul Valenzuda et al. studied the application of ferrites in different fields. He also studied the composite of ferrites with other material. The electromagnetic interference arises due to considerable increase in usage of electronic equipment. The presence of high speed digital interfaces in computers, sensors are passing huge rest of disturbance caused by them. The electric and magnetic field also causes interference in wireless systems. The electromagnetic systems cause disturbance in working of electronic system. This is considered electromagnetic interference. The electric devices usually produce noise at frequency mostly larger compared to signals of circuits. In order to reduce the interference, the particles designed should behave similar to low power

filters. This will enable the circuit to not reject the frequencies higher than given value of frequency [32].

R.C. Chie et al. combines carbon nanomaterial with ferrite. The resulting component showed excellent microwave absorbing properties. The composite of carbon nanotube/cobalt ferrite was prepared by chemical vapor deposition in which cobalt ferrite work as a catalyst. The results showed enhanced microwave absorption. In isolation both are not good absorbers. In case of nanocomposite there is a good plot of magnetic loss and dielectric loss. This happens due to combining ferroelectric material and paramagnetic nanotubes. This will result in improved microwave absorption. The cobalt ferrite nanoparticles, which are dispersed, use resonance phenomenon to absorb signals. Tier shape and nature of interaction enable them to do so. In case of congregated particles all these interactions are not significant [33].

Thi Minh Hue Dang et al. sol-gel hydrothermal method carried out for getting strontium hexaferrite. Different factors effecting synthesis process like mole proportion, Ph, temperature, hydrothermal conditions and process of calcinations were investigated. Rietveld method was used to refine crystal structure. Single crystal phase material was formed having equal Nano size anisotropy was high and shape was plate like. Magnetic coercivity for strontium hexaferrite was measured to be 6.3 kOe and magnetization 11.1 kOe at room temperature. On the basis of strontium hexaferrite other nanoparticles SrLnxFe12-xO19 and $SrFe_{12}O_{19}/CoFe_2O_4$ were synthesize for observation of magnetic phase interaction and crystal structure distortion [34].

Shahid Hussain et al. solid state reaction method was used to check the electrical and structural properties by addition of lead Pb in strontium Sr 0.5Pb0.52+Fe 12-xPbxO19 (x = 0.0, 0.2, 0.4, 0.6, 0.8, 1.0). hematite and Pb multiphase is confirmed from data of XRD. At a temperature of 298-575 K DC resistivity was measured. At 80 Hz to 1 MHz AC conductivity was recorded in same range of frequency dielectric constant and tangent loss are also determined. Hopping model is also used to explain conductivity [35].

Zehra et al. worked on graphene and its composite with hard ferrite to find out microwave absorbing properties. Barium ferrite nanoparticles were prepared by using

sol gel method. They are combining with graphene sheets. Barium hexaferrite nanoparticles were made to deposit on graphene sheets which are of thickness nanometer. The novel composite is prepared to check its microwave absorbing properties. The barium ferrite nanoparticles embedded on graphene has increased absorption. due to layered structure the shielding activity shows much better results. The mechanism involves multiple reflections. Absorption is reason for enhance performance. The physical and structural properties show graphene/barium ferrite to have enhanced microwave absorbing properties [36].

Ibrahim Roohani et al. sol gel was used for the synthesis of SrFe12-xNixO19 for x=0.1.XRD, TEM, VSM and FTIR was used as characterization if samples. Single phase of M type strontium hexaferrite structure was confirmed for $x \leq 0.5$ where for concentration greater than 0.5, NiFe2O4 spinal phase was formed. XRD data was used to calculate crystallite size and lattice parameters as well. Coercivity decreased and saturation magnetization increased by nickel substitution. This study suggests that these materials are good for microwave devices and high density magnetic recording media [37].

2.3 Sol-Gel Method

A gel is formed which is providing homogeneity of high degree and the diffusion if atoms is reduced in the solid state calcination. This technique provided better control on products and costly. The materials which are made through this technique have wide applications in optics, electronics and energy etc.

2.4 Experimental Details

2.4.1 Materials

Strontium nitrates $Sr(NO_3)_2$.

Pure analytical iron nitrate((III) nonahydrate $Fe(NO_3)_3.9H_2O$.

Nickel Nitrate hexahydrate $Ni(NO_3)_2.6H_2O$.

Cobalt Nitrate hexahydrate $Co(NO_3)_2.6H_2O$.

Magnesium Nitrate $Mg(NO_3)_2$.

Lithium Nitrate $Li(NO_3)_2$.

And citric acid ($C_6H_8O_7$) was used. Initial reagent to synthesize all the salts in deionized water. All the chemicals used for samples preparations in this study were of purity ≥ 99% and were used without any further purification.

Ammonia solution for pH.

2.5 Synthesis of Strontium Hexaferrites

$SrFe_{12}O_{19}$ samples were synthesized with use of Sol gel method. This stoichiometric formula is used in order to calculate composition of different chemicals utilized in this process.

Mass= (Molarity, Molecular mass×100)/1000

Solution of strontium nitrates $Sr(NO_3)_2$ and iron nitrate Nona hydrate $Fe(NO_3)_3.9H_2O$ were prepared according to their stoichiometric ratios were dissolved in 200ml of deionized water by constantly stirring using a magnetic stirrer for 15 minutes for their complete dissolution and to get clear solution in water.100 ml of deionized water was taken to dissolve citric acid and was stirred until solution get cleared and complete dissolution took place. In a large beaker both solutions were added with continuous stirring using a magnetic stirrer after 15 minutes of stirring ammonia was then added by drop by drop method until pH rise to 7.

After that system is then kept under continuous stirring with a magnetic stirrer and now heating at 350-degree centigrade temperature is powered ON, with the same condition of stirring. After sometime the solution starts to change in gel form, after that the gel solution then catches fire and after the complete combustion the heating and stirring is stopped.

Finally, a powder was obtained which was of dark color. This powder was grinded in mortar and pestle and then it was kept in the muffle furnace at 950 °C for 3 hours for calcination purpose.

2.5.1 Synthesis of $SrFe_{12}O_{19}$ with Co, Mg and Li Dopant

Series of sample preparation with cobalt, lithium and magnesium as a dopant was prepared. The series is $SrFe_{(12-3x)}(Co,Mg,Li)_xO_{19}$ for x=0.15,0.25,0.5, were prepared. Samples were prepared in 400 ml of deionized water by adding $Sr(NO_3)_2$, Fe $(NO_3)_3.9H_2O$, Co $(NO_3)_2$. $LINO_3.Mg(NO_3)_2.6H_2O$ and citric acid according to their stoichiometric ratios by sol gel technique. The solution was continuously stirred for 15 minutes with magnetic stirrer until the complete dissolution took place solution

becomes clear. Ammonia solution was dropped by drop by drop method until the Ph reaches 7 with continuous stirring.

The system is than kept under constant stirring with a magnetic stirrer and now heating at 350-degree centigrade temperature is powered on with the same condition of stirring. After sometime the solution starts to in gel form, after the gel solution catches fire in the beaker and after the complete combustion the heating and stirring is stopped. Finally, powder was obtained which is of dark color. This powder is then finely grinded in mortar and pestle and then was placed in muffle furnace at 950 degrees centigrade for calcination purpose.

1) Deionized water

2) All salts added in deionized water

3) Adding ammonia

4) heating

5) Grinded powder

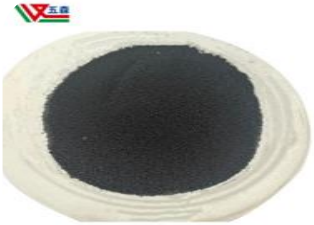

6) After annealing

Fig 2.1 Step by step Sol-gel process [38]

2.6 Sample Preparation

Samples were prepared using different methods for the measurement of SEM, FTIR, electric and magnetic properties. Procedures, use for the preparation of different samples are discussed under:

2.6.1 Preparation of SEM Samples:

SEM is used for the study of surface morphology and for getting 3D images of surface. A very small amount of powdered material was dispersed in water using ultrasonicator for about one hour and then drop of mixture is dripped on a clean substrate. On substrate surface powder particles are dried and dispersed for further processed of analysis by SEM.

2.6.2 Preparation of FTIR Samples

Kbr pallet method was used for sample preparation because alkali salts give no absorption in IR spectrum. Potassium salt was placed in oven at 100 degrees centigrade for one hour for removal of moisture. Small amount of sample and Kbr was taken and ground to fine powder and pallet was prepared using pallet die set and hydraulic press. Mixture of ground and Kbr and sample was added into the die and it was then placed into the press and with the pumping movement, moved the hydraulic pump handle downwards until it shows 3 tones on the scale. Waited for forty-five seconds, pressure was released and die was taken out. Finally, a thin sample pallet having thickness in the range of 2-3 mm and die of 13mm was obtained.

2.6.3 Preparation of Samples for Measurement of Electrical Properties

For measurement of electrical properties of samples, pellet for each sample was prepared. Pellet was prepared using pellet die set and hydraulic press. Each sample was finally grinded before sample preparation. Pellets were prepared using 1 gram of each. Pellets prepared were measured using Vernier calliper and found almost some thickness and diameter (2mm thickness and about 10 mm diameter) for all pallets. By the use of hydraulic press for applying a load of 4 tons for 2 minutes on each pallet. The prepared pallets were kept at 800 degrees centigrade to be sintered for 2 hours and used for measuring electrical properties. (dielectric constant and dielectric loss)[38].

Fig 2.2 pellets of ferrites [38]

Chapter 3

Introduction to Sample Characterization Techniques

The characterization refers to broad and general process by which a material's structure and properties are probed and measured. The properties of synthesized strontium hexaferrites nanoparticles with cobalt, magnesium and lithium loadings are analyzed by performing some specific analysis techniques. Properties like physical and chemical properties and other information about material such as morphology, lattice parameter, structure etc. can be obtained using one of the analysis technique. Following characterization techniques can be used for the analysis of synthesized composite.

3.1 X-Ray Diffraction Technique

X-ray diffraction is a non-destructive technique for characterizing the crystalline materials. It provides information on the structure, phases, preferred crystal orientations(texture), and other structural parameters such as average grain size, crystallinity, strain and crystal defects. Three different methods can be used to find out crystal structure i.e. powder diffraction method, Laue method, and rotating crystal method. Two methods can be used to determine crystallite size if powder diffraction method is used. Those techniques are as follows:

- Debye sherrer method.
- Diffractometer method.

The sample was in the form of fine grinded powder. Copper, molybdenum etc. can be used as a target material [39].

3.2 Basic Principle for XRD

The powdered sample is placed fir analysis. X ray beam is made to fall on the sample and reflected from plane of crystal. The crystal planes reflect the x rays that are incident on material. The interference only takes place when the incident angle is exactly same as reflection angle. The bragg's law is given by

$n\lambda = 2d\sin\theta$…… (1)

n is the order of interference, θ is the angle of incidence is the interlayer distance and λ is incident X-ray wavelength. The bragg's law states that the incident ray is reflected only when the path length difference between set of planes is 2dsinθ. The set of planes are at equal distance of d. following is the condition required for constructive interference:

$2d\sin\theta = n\lambda$, where n=1,2,3……

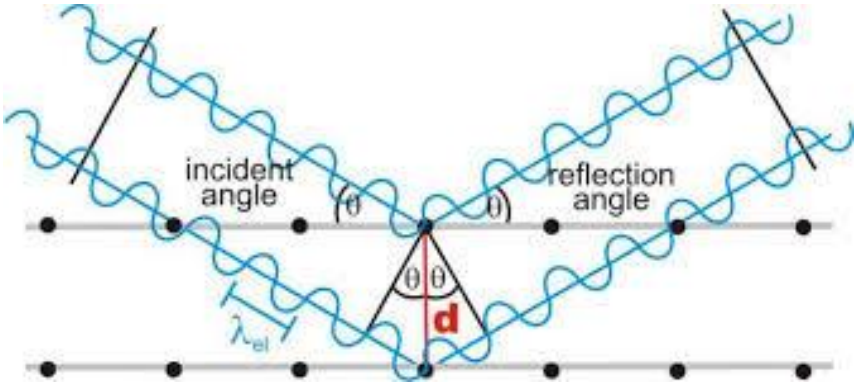

Fig 3.1 Incident x ray beam scattered by atomic plane in a crystal [39]

This equation is known as bragg's equation. The condition for reflect ion mention in above equation is that it only occur when $\theta < 2d$. for this reason visible light cannot be used. For characterization of a three dimensional structure three techniques are usually used which are as follows:

- Laue method.
- Powder method.
- Rotating crystal method.

The sample which is used to be characterized using XRD is in the form of Nano powder.so the powder method will be the one useful for the desired sample. For the evaluation of powdered sample and in the case of in availability of single crystal of acceptable size, powder diffraction is the best method to be employed. The procedure of this experiment involves the crushing of sample into fine powder. Afterwards the sample will be placed into aluminium or glass rectangular shaped plate. A monochromatic X ray beam is than directed towards the powdered sample [40].

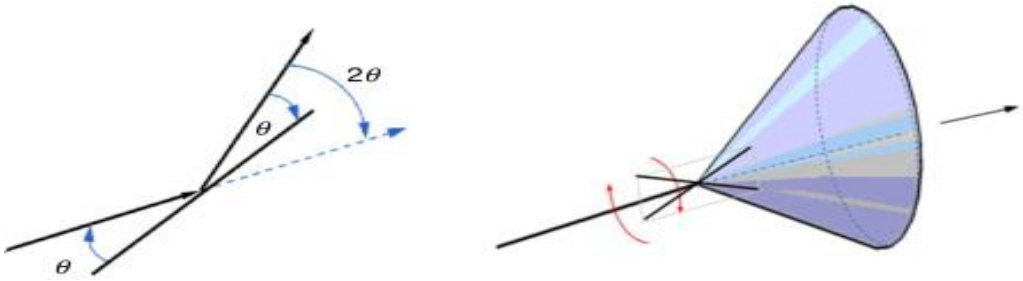

Fig 3.2 Diffracted cones of radiations forming in powder method [40]

Consider the reflection as shown in figure. The fraction of sample, which is in powder form, is at such an orientation which will enable reflection by being present at correct bragg angles. When the plane is rotated about the beam, which is made incident, the path of motion of reflected beams will be across the surface of cone. In the case of our particles, the reflection does not occur across the surface, a large number of crystal particles will have same reflections and some of those reflections will be able to satisfy bragg's law. The inter planner kl spacing, d can be calculated by knowing values of λ and θ.

3.3 Lattice Constant

Lattice constant defines the unit cell of a crystal.it is the length of on edge of a cell or angle forming between the edges. It can also be termed as lattice constant or lattice parameter. The distance, which is constant, between the lattice points is known as lattice constant. Following equation is used to calculate lattice constant.

$$a \frac{=(h^2+k^2+l^2)½}{nsin\theta} \ldots\ldots\ldots\ldots\ldots 3.2$$

In above equation lattice constant is a, the wavelength of X-ray radiation is 1.54 A° for CUKα, miller indices are h, k, l and diffraction angle is θ radian or degree [40].

3.4 Crystallite Size

For the identification and confirmation of the experimentally obtained diffraction pattern it is compared to JCPDS cards. The structural properties are greatly influenced by particle size. According to Debye sherrer equation, which is used to calculate particle size, crystal size is inversely proportional to peak width. So the small crystallite size is relayed to peak broadening in XRD analysis. The Debye sherrer equation is used to calculate particle size.

$$t=\frac{0.9\lambda}{\beta cos\theta} \quad \text{.....(3.3)}$$

λ represents the incident x ray wavelength and θ and $\boldsymbol{\beta}$ represents diffraction angle and full width half maximum respectively [40].

3.5 X-Ray Density

The x ray diffraction data can be used for calculation of sample's material density. If the lattice constant is known for each sample following formula is used.

$$\rho x =\frac{8M}{Na^3} \quad \text{.....(3.4)}$$

where M represents molecular weight of sample is the Avogadro's number ($6.02*10^{23}$) and a is the lattice constant. Eight formula units are processed by each cell [40].

- **Measured Density**

The intrinsic properties of material define the bulk density or measured density. The density formula is generally used for the density calculation.

$$\rho m=\frac{m}{\pi r^2 h} \quad \text{.....(3.5)}$$

where m represents the mass, r represents the radius, h is the thickness of pressed pallet sample. For the calculation of measured density, a circular pallet is made, using hydraulic press which compacts the powdered sample. Vernier caliper is used to measure thickness and radius of pallet and analytical balance is used for measuring mass of the pallet. The measured parameters are substituted in equation for resultant density calculation [40].

- **Porosity Fraction**

Along with the alternation in compositions, the increase in the porosity fraction is observed. Following formula is used for calculation of porosity fraction.

Porosity fraction=I-$\frac{pm}{px}$……(3.6)

3.6 Scanning Electron Microscopy

Scanning electron microscopy is an imaging technique which makes use of high energy electron beams for imaging Nano and bulk surfaces. When the highly energetic beams strike the sample surface it provides following information.

- Composition of the sample.
- Phase mapping.
- Topography of the sample.

When the beam hits the surface of the material there will be various kinds of interactions and signals are emitted as a result of these interactions such as transmitted electrons, back scattered electrons, secondary electrons, cathodoluminiscence, and characteristic X-rays [41].

3.6.1 Basic Principle of SEM

The beam of electrons is made to focus on the surface of the sample in scanning electron microscopy. The faster scan is used which can focus on very narrow cross sectional area. The surface of the sample will emit electron or photons when the incident electron beam interacts with the surface. Different sets of detectors are employed to collect the emitted photons or electrons. The brightness of the cathode ray tube is controlled by using the outputs of detectors. The x and y input of cathode ray tube are adjusted in relation with X and Y voltages restring the beam of electron. As a result, image is obtained on cathode ray tube display. Images are produced by back scattered electrons, elemental X rays and secondary electrons [41].

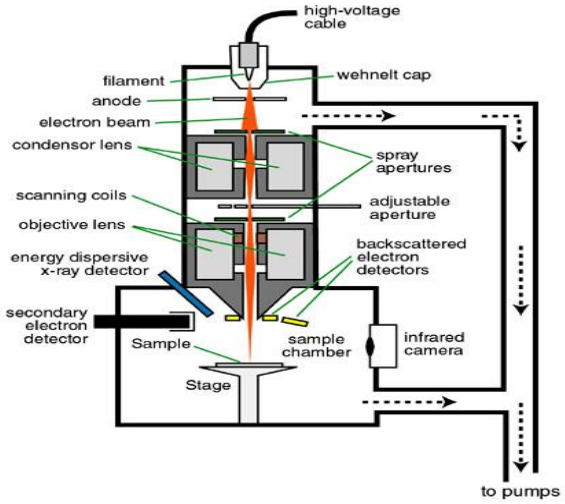

Fig 3.3 Schematic figure of Scanning Electron Microscope [41]

3.7 Fourier Transform Infra-Red Spectroscopy

The absorption, emission spectra's, Raman scattering and photoconductivity of the material can be obtained by using this analytical technique. The stretching modes of the elements present in composite and chemical purity of the sample can be determined using FTIR. Kit is known as FTIR because it involves the Fourier, a mathematical term. It collects the data from spectrum of matter. FTIR is used to determine the amount of light that a sample absorbs at a specific wavelength [41].

3.7.1 Working Principle of FTIR

In FTIR, an infra-red light beam from the source which is polychromatic is made to fall on the splitters. Half of the portion of the incident light is refracted towards the fixed mirror and other half of the incident light is then transmitted through a mirror which is movable. Transmitted light is passed through the sample. The information about molecular component and structure of the sample can be obtained by interaction of light with sample.

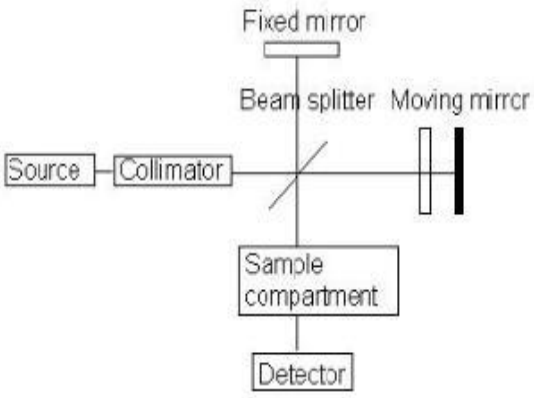

Fig 3.4 Schematic figure of FTIR Spectroscopy [41]

It is a sensitive technique and can also be used for identification of many organic compounds for example paints, polymer, resins, coatings and drugs etc. it is the only analytical technique which provides ambient temperature operation and capability of monitoring the vibrations of functional group directly, which is used for characterizing molecular structure and governing the course according to the principle of FTIR, molecular vibrations are produced because of absorption of IR radiations when applied IR frequency is equal to the natural frequency of vibration. Different frequencies are required by every different blonds or functional groups for absorption. Therefore, the characteristic peak is observed for every functional group or part of the molecule.

3.7.2 Applications of FTIR

The components of a mixture are separated using gas chromatography.

- The analysis of liquid chromatography fraction can be done using FTIR.
- The samples can be checked with the help of infra-red microscope in sample chamber.
- The sample having emitted spectrum of light is obtained by FTIR in place of light spectrum through the sample [41].

3.8 Electrical Properties

Dielectric properties are measured using impedance analyzer. Pallet is placed in pallet holder and connected to device [41].

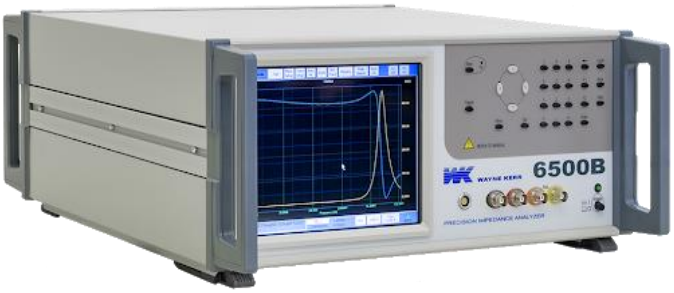

Fig 3.5 Schematic figure Impedance analyzer [41]

3.8.1 Dielectric Properties

The LCR meter bridge is useful for determination of the dielectric properties such as dielectric loss, dielectric constant etc. Firstly, the capacitance of pallets was find out using LCR meter then following formula is used for the calculation of dielectric constant.

$$\acute{\varepsilon}=\frac{cxd}{\varepsilon_0 A} \quad \text{.....(3.7)}$$

where C represents the capacitance of the pallet (farad), t represents the thickness of the pallet (meters), A represents the cross sectional area of the flat surface of the pallet, and ε0 is the constant of permittivity of free space, and its value is $8.85*10^{-12}$ F/m. The imaginary part that corresponds to energy dissipation losses is calculated by using the following equation.

$$\varepsilon'' = \varepsilon'*D \quad \text{..... (3.8)}$$

there will be some power losses in dielectric materials. These losses are due to the work done in order to overcome frictional and damping forces faced by dipoles during their rotatory motion. The dielectric loss tangent can be find out by using following equation.

$$\tan\delta=D=\frac{\varepsilon''}{\varepsilon'} \quad \text{.....(3.9)}$$

following equation is used for calculation of AC conductivity.

$$\sigma ac=\omega\epsilon\epsilon o\tan\delta \quad \text{..... (3.10)}$$

3.8.2 AC Impedance Spectroscopy

The AC impedance parameters of the samples were measured at room temperature. Resistance (R) and reactance (X) were measured over the frequency range of 100 Hz to 5 MHz. the impedance is a complex quantity where resistance (R) and reactance (X) shows the real part and imaginary part of impedance in the circuit by relation:

$Z = R + j\,X$……... (3.11)

The impedance Clot plot shows the resistivity of the material the SI unit of impedance is 'Ω' where resistance (R) and reactance (X) shows the real and imaginary part of the impedance shows the contribution of resistance in the material by the relation:

$Z' = R = |Z|\cos\theta z$……... (3.12)

$Z'' = X = |Z|\sin\theta z$……... (3.13)

The impedance shows the resistive behavior of the material [41].

3.8.3 Electric Modulus

The real and imaginary part of the electric modulus M' and M" respectively can be calculated as follows:

$M' = \frac{\acute{\varepsilon}}{(\acute{\varepsilon}2+\varepsilon''2)}$……..(3.14)

$M'' = \frac{\acute{\varepsilon}}{(\acute{\varepsilon}2+\varepsilon''2)}$……..(3.15)

In above expressions έ and ε" is the real and imaginary part of dielectric constant respectively.

3.8.4 Two probe method

Ohm's law is used for the study of electrical properties such as conductivity and resistivity. The decrease in resistance with increase in temperature of semiconductors tells about conductive nature of materials.

Ferrite pallet is used in sample holder for measuring the current. By using ohm's law resistance is calculated from the values of current and voltage.

$V = IR$…… (3.16)

$R = \frac{V}{I}$……(3.17)

From the values of resistance, resistivity is measured at different values of temperature.

$\rho = RA/L$……(3.18)

where R is the resistance, A is the area and L is the thickness of pallet. Resistivity increases with increase in resistance and area. Whereas increase in thickness decrease resistivity. Decrease in resistivity means decrease in conductivity [41].

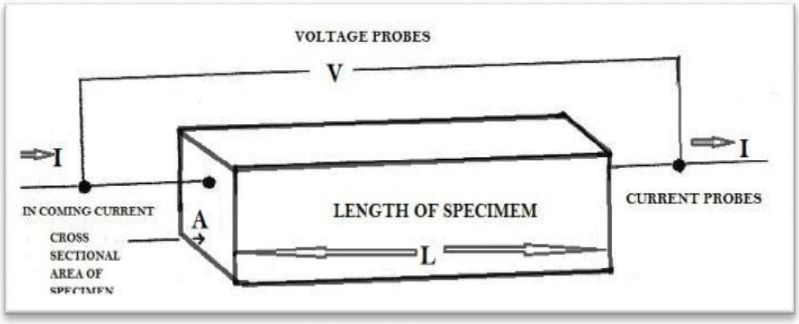

Fig 3.6 Schematic figure of two probe method [41]

The temperature is varied from 100 to 280 degree centigrade. The variation in conductivity and resistivity tells about conductive nature of sample.

Drift mobility is calculated by using following equation:

$\mu d = \frac{1}{ne\rho}$…….. (3.19)

$n = \frac{N_a F_e D_b}{M}$…… (3.20)

Here NA called the Avogadro's number, PFe is a no of iron atoms which are in chemical formula, DB is the bulk density of sample, M is the Molar mass.

Measurements are taken at room temperature. The temperature difference of 10 degrees centigrade is given. By varying temperature, the current changes and different values of resistance are measured that are used to find resistivity and mobility. From these values the conductive nature of sample can be determined.

KEITHLEY is a software used to measure current at different voltages. This instrument is brought into working by optimizing it at different values of voltages and current. After a lot of work and testing of different samples. This system is now functional and can be used to measure values of current by varying the values of

temperature. Voltage from 1 to 50 volts is varied and different values were calculated. Current variation with voltage and temperature is observed and studied for the optimization of setup maximum current was given and temperature up to 240 degrees centigrade was given and behavior of materials was observed. This setup is usually used to study the electrical and conductive behavior of samples at different conditions. Voltage can be given up to 50 V with changing current and limits [41].

Chapter 4

Results and Discussions

4.1 X-Ray Diffraction Results

The knowledge of formation of phases and study of the structure was found out using XRD. The sample which was prepared was then finely grounded and annealed before subjecting it to XRD.

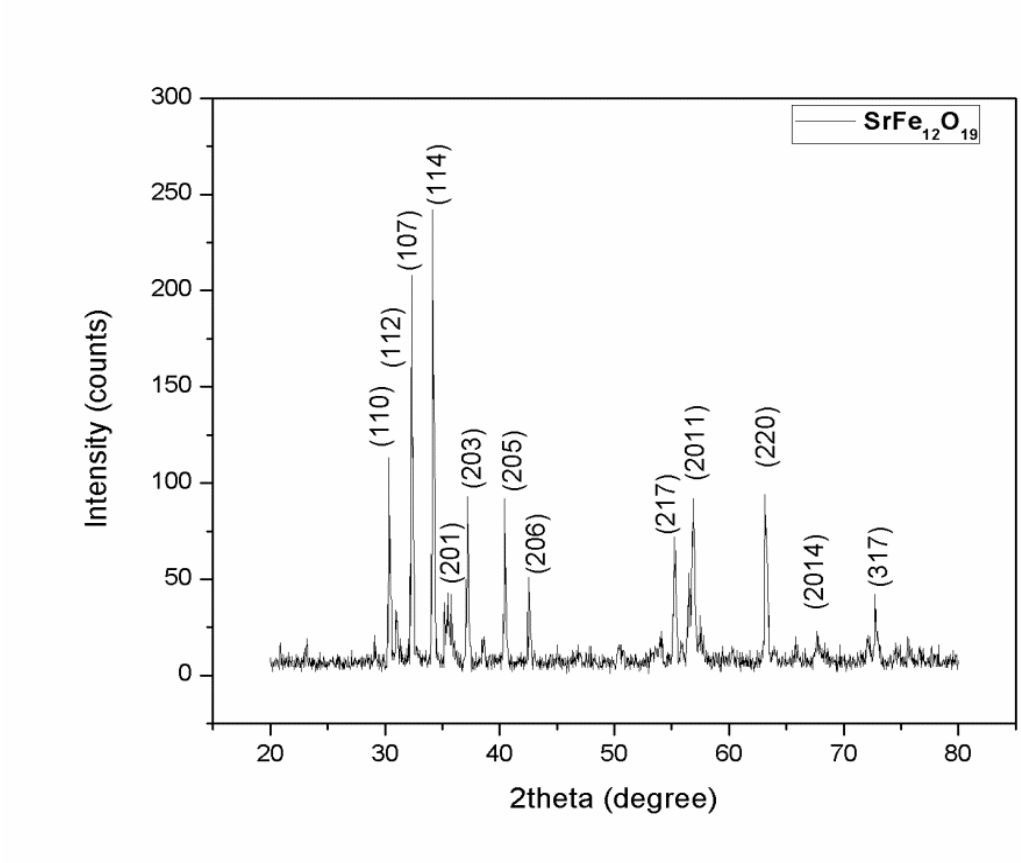

Fig 4.1 XRD pattern of pure strontium hexaferrite

Fig 4.1 shows the obtained XRD pattern at room temperature. The peaks which are nicely separated, their diffraction appears for all the samples at planes (1 1 0), (1 1 2), (1 0 7), (1 1 4), (2 0 1), (2 0 3), (2 0 5), (2 0 6), (2 1 7), (2 0 11), (2 2 0), (2 0 14) and (3 1 7) which are present at all respective angles of 2θ=30.358, 31.359, 32.356, 34.197, 35.43, 37.1524, 40.425, 42.553, 55.218, 56.868, 63.17, 67.733 and 72.768. The existence of these peaks at some specific angles verifies the generation to the card

number JCPDS 01-080-1197. There is no secondary peak present for hematite which is an extra phase hence this shows the completion of the reaction.

1.1.1 Co, Mg and Li Substituted Hexaferrites $SrFe_{(12-3x)}(Co,Mg,Li)_xO_{19}$

The XRD pattern of all three compositions of Co, Mg, Li substituted strontium hexaferrites having compositions x=0, x=0.15, x=0.25, x=0.5 were synthesized by using by using sol gel method as shown in fig 4.2. Miller indices corresponding to the XRD peaks for the compounds synthesized are comparable exactly with the standard one of strontium hexaferrite JCPDS 01-080-1197 indicating the single hexagonal phase structure of these samples. These powder samples with the substitution of Co, Mg, Li shows that the cations which are doped slightly alter the value of the lattice parameter probably because of slight change in ionic radii of metallic cations and iron. The ionic radii of Fe^{+3} is 0.60A^o while the ionic radii of Co, Mg and Li is 0.70 A^o,0.65 A^o,0.70 A^o respectively. so, as the ionic radii of three metallic cations and iron were comparable suggesting that the cations replaced iron-on tetrahedral sites. The phase of extra hematite is then formed due to Dopant and then increases with the concentration of Doping.

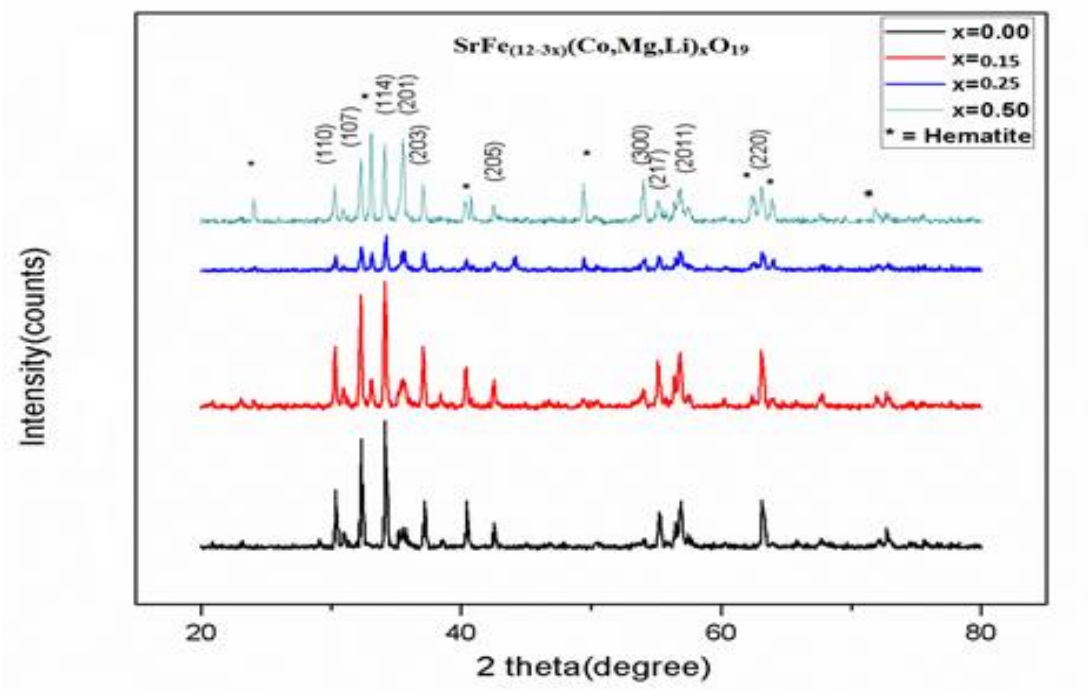

Fig 4.2 XRD pattern of Co, Mg and Li doped strontium hexaferrite

4.2 Scanning Electron Microscopy Results

Scanning electron microscope is used to find out $SrFe_{12}O_{19}$ nanoparticle size and morphology. The results are shown here. The results include pure $SrFe_{12}O_{19}$. For the morphology analysis of pure strontium hexaferrite, Co, Mg, Li doped ferrite, all powders were then annealed and a suspension in the deionized water was made using the sonication process. This will allow the Nano particles to arrange themselves in lowest interface energy configuration. Results shows uniform distribution of strontium hexaferrites nanoparticles. The nanoparticles are thus fairly distinguished and separated from one another and their size ranges from 15 nm to 20 nm.

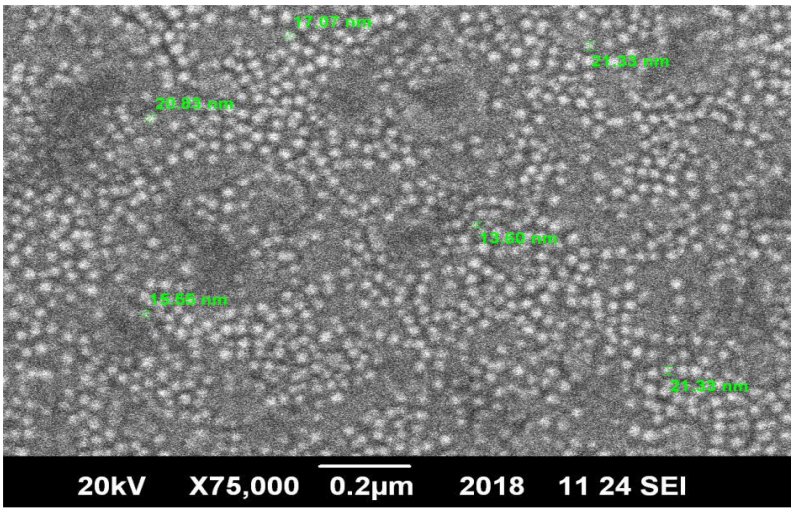

Fig 4.3 SEM image of pure strontium hexaferrite

The SEM image of pure strontium hexaferrite shows the spherical nanoparticles. The result shows there is no agglomeration. Uniform distribution can be seen clearly without presence of any impurity. It has been seen clearly that nanoparticles are homogeneously distributed and uniform. The results can include $SrFe_{(12-3x)}(Co,Mg,Li)_xO_{19}$ with x=0.0, x=0.15, x=0.25, x=0.5. for morphological analysis of Co, Mg, Li doped strontium hexaferrite, all of the powders were then annealed and a suspension was made in deionized water using Sonication process. Their size ranges from 18 nm to 31 nm. There is no change of size when increasing the concentration of Co, Mg and Li due to grain boundaries.

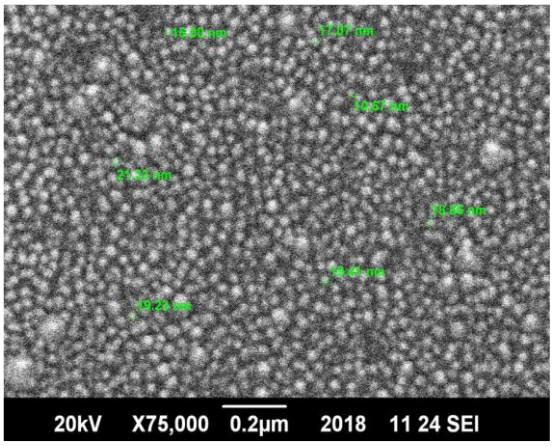

Fig 4.4 SEM image of $SrFe_{(12-3x)}(Co,Mg,Li)_xO_{19}$ for x=0.15

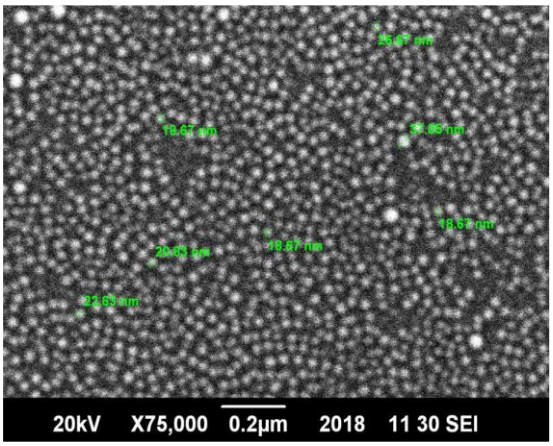

Fig 4.5 SEM image of $SrFe_{(12-3x)}(Co,Mg,Li)_xO_{19}$ for x=0.25

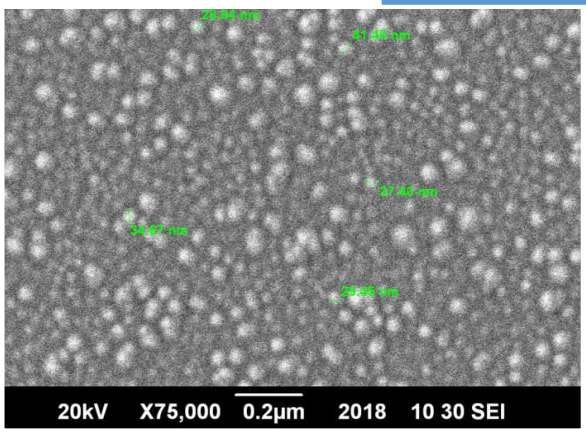

Fig 4.6 SEM image of $SrFe_{(12-3x)}(Co,Mg,Li)_xO_{19}$ for x=0.5

4.3 Fourier Transform Infra-Red Spectroscopy Results

Fig 4.7 shows the FTIR analysis of pure strontium hexaferrite. The KBr pallet is used and analysis is performed at room temperature in the range of 300 cm^{-1} to 1400 cm^{-1}. It can be inferred from FTIR results that the same kind of chemical bonds are present in all the samples as the spectra shown by all the samples are nearly undifferentiated. In ferrites the two sub lattice positions occupied by metal ions are tetrahedral and octahedral positions. Vibration modes of tetrahedral are higher than octahedral. Metal and oxygen bonds are there that form crystal structure. The bands at 433.19 cm^{-1} to

592.36 cm^{-1} represent metal vibration in octahedral and tetrahedral complexes. These bands are due to stretching of tetrahedral and octahedral lattice sites. Absorption bands appear as a result of stretching and vibration of metal-oxygen bonds at both lattice sites. Due to the variation in bond lengths of Fe-O, the positions of bands differs slightly from each other at both tetrahedral and octahedral lattice sites.

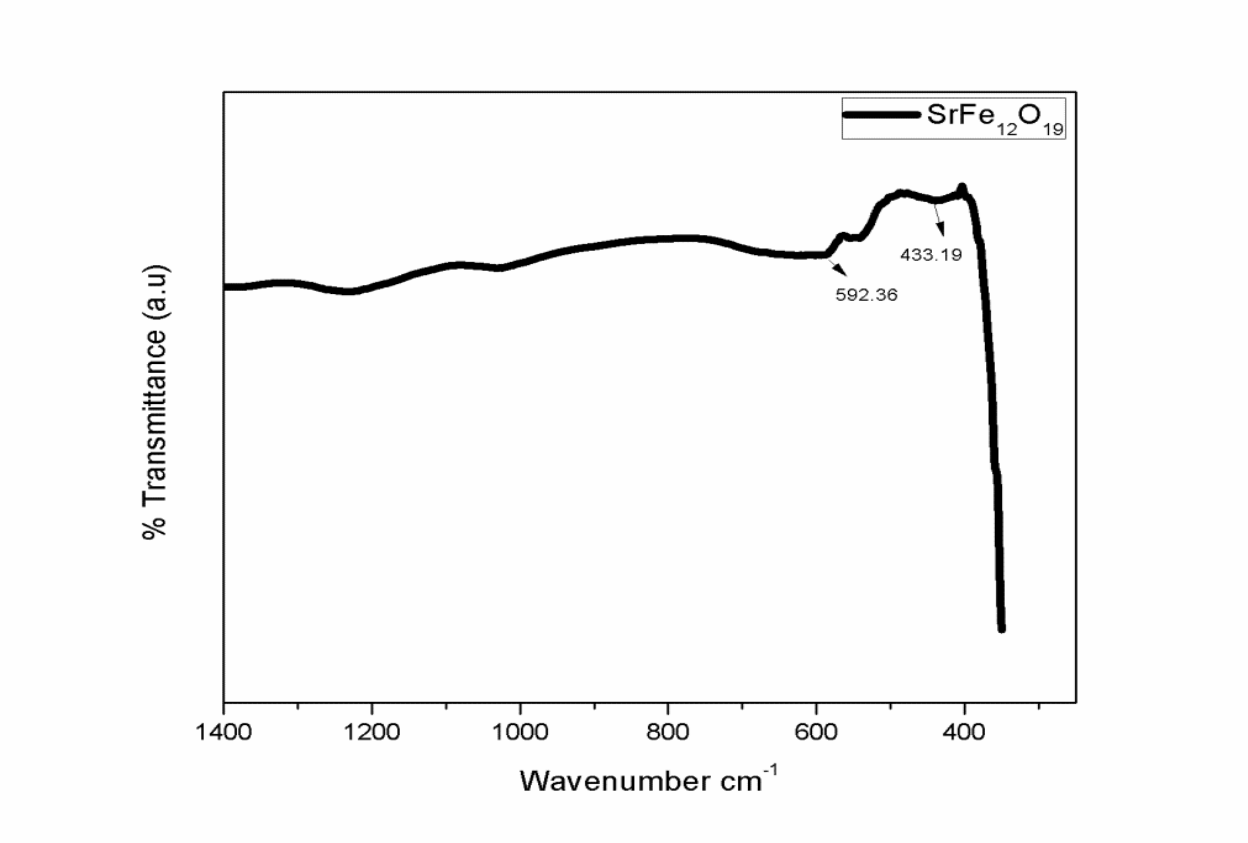

Fig 4.7 FTIR spectra of pure strontium hexaferrite

Fig 4.8 shows the FTIR analysis of Co, Mg, Li doped strontium hexaferrite. The KBr pallet is used and analysis is performed at room temperature in the range of 300 cm^{-1} to 1400 cm^{-1}. It can be inferred from FTIR results that the same kind of chemical bonds are present in all the samples as the spectra shown by all the samples are nearly undifferentiated. In ferrites the two sub lattice positions occupied by metal ions are tetrahedral and octahedral positions. Vibration modes of tetrahedral are higher than octahedral. The sub lattice positions give rise to absorption bands. All organic compounds are burnt at calcination temperature of 950^0C as no peak is present for other organic compounds. Metal and oxygen bonds are there that form crystal structure. The bands at 430 cm^{-1} to 597 cm^{-1} represent metal vibration in octahedral and tetrahedral complexes. These bands are due to stretching of tetrahedral and

octahedral lattice sites. Absorption bands appear as a result of stretching and vibration of metal-oxygen bonds at both lattice sites. Due to variation in bond lengths of Fe-O, the position of bands differs slightly from each other at both tetrahedral and octahedral lattice sites. The shifting of peaks to higher wavenumbers by Co, Mg, Li doping is due to lower atomic weight of Co^{2+}, Mg^{2+}, Li^{2+} there is inverse relation between atomic weight and wave number.

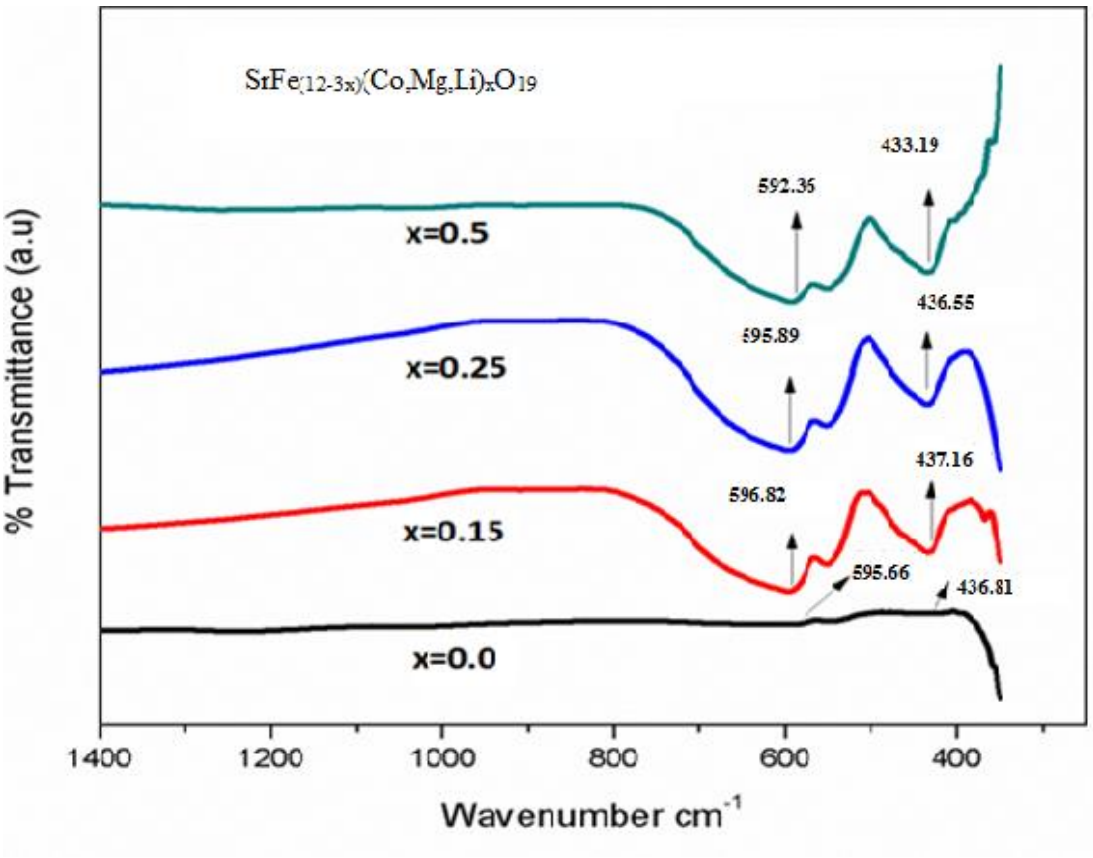

Fig 4.8 FTIR spectra of Co, Mg, Li doped strontium hexaferrite

4.4 Dielectric Studies

To find out the dependence of dielectric constant. Dielectric loss, tan loss, AC conductivity and Ac impedance on frequency, pallets were prepared and sintered and standard relations are used for calculations.

4.4.1 Dielectric Constant

The Dielectric constant has a real part and imaginary part. The value of the dielectric constant is higher at lower frequencies. Pure strontium hexaferrite has 16.9 value of dielectric constant at 250 Hz. However, in case of Co, Mg, Li doped strontium hexaferrite dielectric constant increases by increasing. Co, Mg and Li concentration as shown in fig. dielectric constant is 77.8 for x=0.5.

The increase of dielectric constant values at lower frequencies can be well explained by Maxwell and Wagner model of space charge polarization [37]. According to this model, a dielectric material is divided into two parts, grains and grain boundaries. Grains are considered to be relatively conductive while grain boundaries are highly resistive. When an external field is applied, the electrons start to move toward grain boundaries. Accumulation of electrons happens at the grain boundaries because of the resistive nature of boundaries and result in the polarization of material.

At higher frequencies, a slow response is shown by these charge carries which result in decrease in space charge polarization and ultimately low values of dielectric constant. Trend of the dielectric constant at 250 Hz frequency is shown in fig 4.10 below that shows an increasing trend.

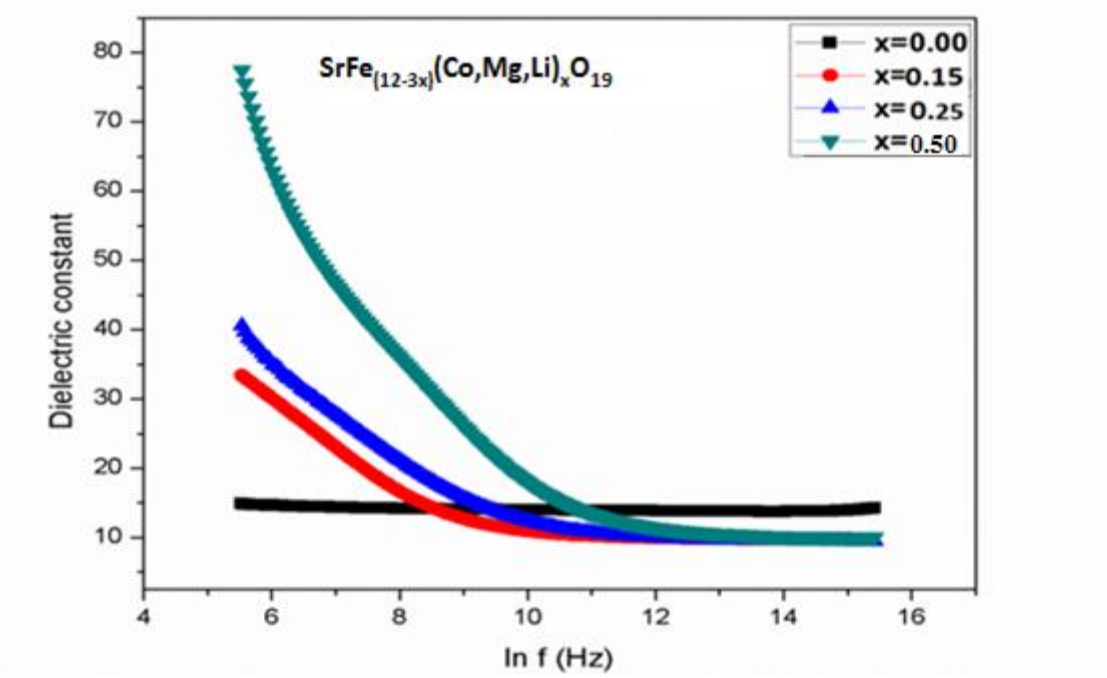

Fig 4.9 Dielectric constant variation with frequency for $SrFe_{(12-3x)}(Co,Mg,Li)_xO_{19}$

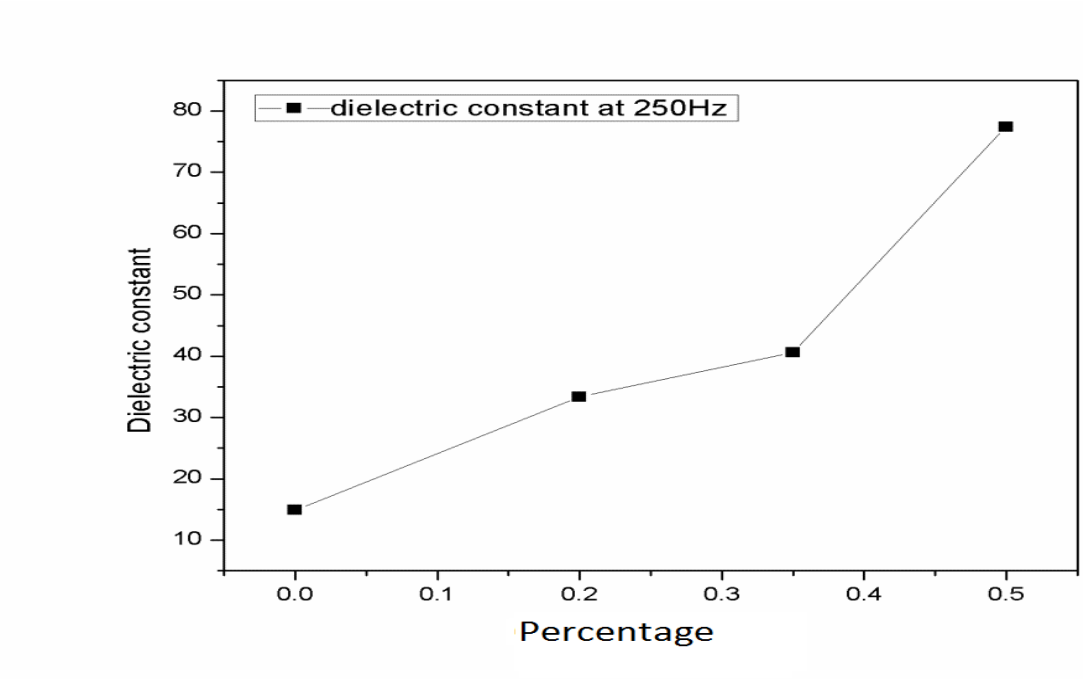

Fig 4.10 Dielectric constant variation at 250 HZ for $SrFe_{(12-3x)}(Co,Mg,Li)_xO_{19}$

4.4.2 Dielectric Loss

Dielectric loss is a part of dielectric constant which is imaginary that deals with the amount of energy which is dissolute.

The value of the Dielectric loss is high at lower Frequencies and its value is decreased as Frequency increases. The value rises from 2.21 for pure strontium hexaferrite sample to 54.1 for sample having maximum concentration of Co, Mg, Li in $SrFe_{(12-3x)}(Co,Mg,Li)_xO_{19}$ for x=0.5.

The decreasing behavior of dielectric loss at higher frequencies can be explained by Koop's theory. According to this theory, polarization requires more energy in low frequency regions because of highly resistive grain boundaries. Hence energy losses are high. Whereas, resistivity of grain boundaries in high frequency region is relatively lower so the polarization of material become slight easy. Hence the dielectric losses start to decrease.

Dielectric loss shows increasing trend at 250Hz frequent as shown in fig 4.12. dielectric loss has a value of 1.11 for pure strontium hexaferrite when x=0.00 for $SrFe_{(12-3x)}$ (Co, Mg, Li)$_xO_{19}$, this value of dielectric loss increase to 13.11 when x=0.15,

this value further increases to 20.58 for x=0.25, dielectric loss rises to maximum value of 51.77 when x=0.5 at 250 Hz frequency.

The energy loses in $SrFe_{(12-3x)}(Co, Mg, Li)_xO_{19}$ for the value of x=0.5 is, maximum it requires a greater amount of energy for polarization, x=0.25 requires greater value for polarization then x=0.15. polarization for pure samples is least due to its less energy dissipation.

Materials with higher value of dielectric constant have a higher value of Dielectric loss as well. By increase in frequency the dielectric loss decreases, the grain boundaries are not resistive where frequency is higher. The energy loss for pure sample is less as compared to having samples having Co, Mg, Li contents. As the amounts of Co, Mg, Li increases in strontium hexaferrite the energy loss increases. These materials are very good for energy storage devices.

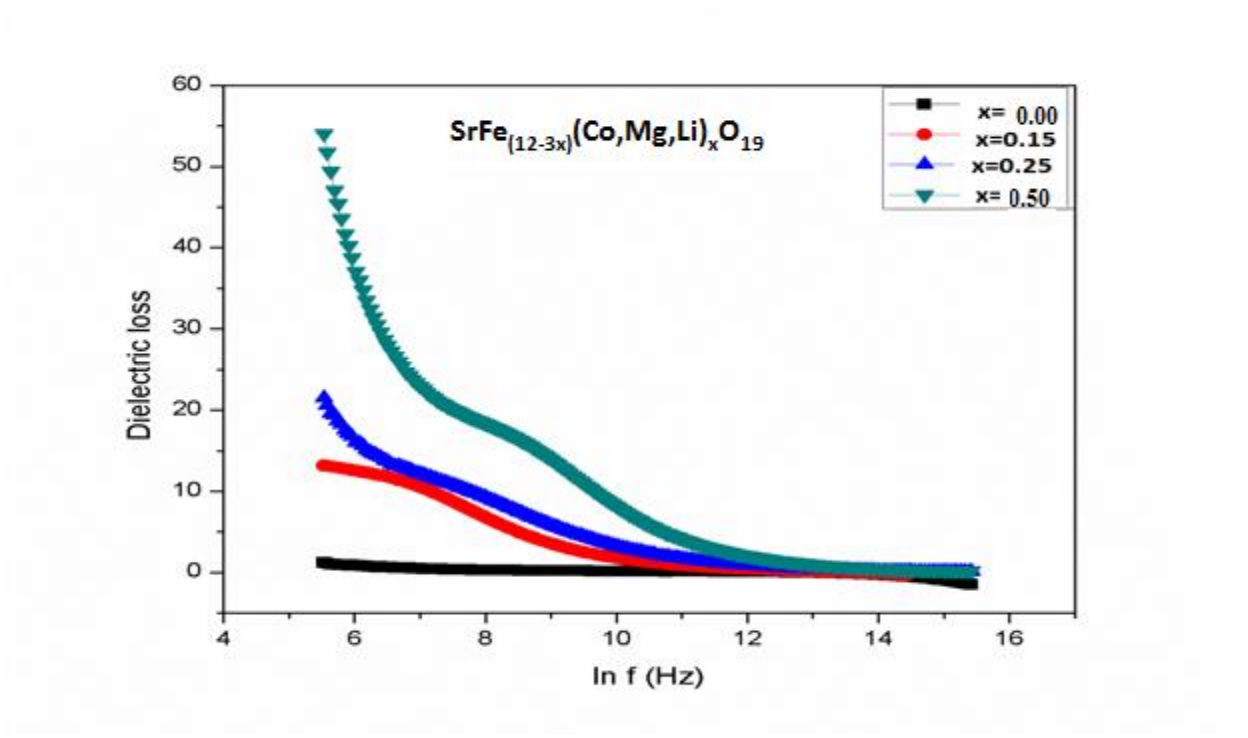

Fig 4.11 Dielectric loss variation with frequency for $SrFe_{(12-3x)}(Co,Mg,Li)_xO_{19}$

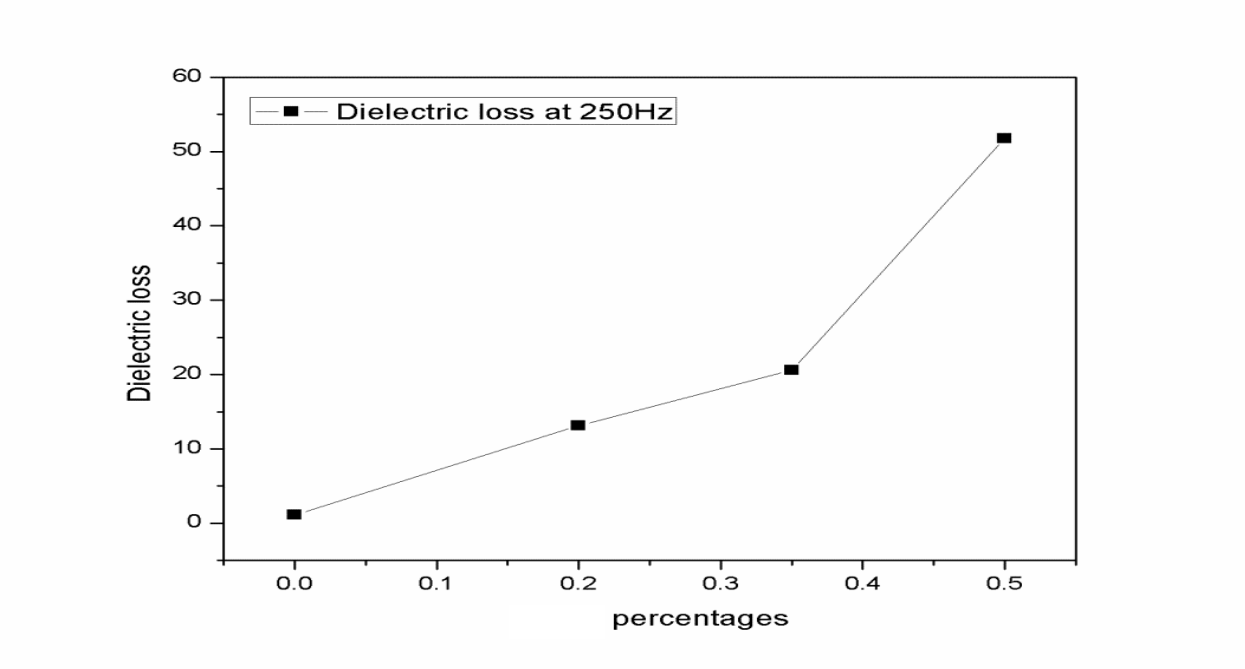

Fig 4.12 Dielectric loss variation at 250 Hz for $SrFe_{(12-3x)}(Co,Mg,Li)_xO_{19}$

4.4.3 Dielectric Tangent Loss

The ratio of dielectric loss to dielectric constant Is given by tangent loss. It quantifies the relative energy loss across a large frequency range due to varying electric field. The Dielectric tangent loss shows a trend which is decreasing with increase in Frequency.

The increase in Co, Mg, Li contents in strontium hexaferrite will give higher values of dielectric tangent loss at low frequencies. The tangent loss increases by increasing value of x for $SrFe_{(12-3x)}(Co,\ Mg,\ Li)_xO_{19}$ in fig 4.19. by increase in Co, Mg, Li concentration tangent loss factor increases from 0.15 for x=0.00, 0.35 for x=0.15,0.50 for x=0.25 and 0.75 when x=0.5.

From the results and values of dielectric constant and dielectric loss decrease in values with increase in frequency is seen. The Dielectric tangent loss is a ratio of the Dielectric loss to Dielectric constant, a decrease in tangent loss is seen with increase in frequency. Whereas there is increase in tangent loss of strontium hexaferrite by doping of Co, Mg and Li. By increasing the concentration of Co, Mg and Li, the values of tangent loss are observed. It is the energy loss due to varying electric field. Energy

loss increases with increase in Co, Mg and Li content. At higher frequencies/ relative energy loss is observed.

The increase in Dielectric tangent loss values are in accordance with Koop's theory. The theory explains that at lower frequencies the hopping of electrons is high. The hopping decreases at higher frequencies.

The fig shows the variation of dielectric tangent loss at the frequency of 250 Hz for $SrFe_{(12-3x)}(Co, Mg, Li)_xO_{19}$. The value is 0.15 for pure strontium hexaferrite x=0 this value increased to 0.35 when Co, Mg and Li is added for x=0.15 then increases to 0.54 for x=0.25 and for x=0.5 dielectric tangent loss increases to maximum value of 0.73 by addition of Co, Mg, Li in pure strontium hexaferrite.

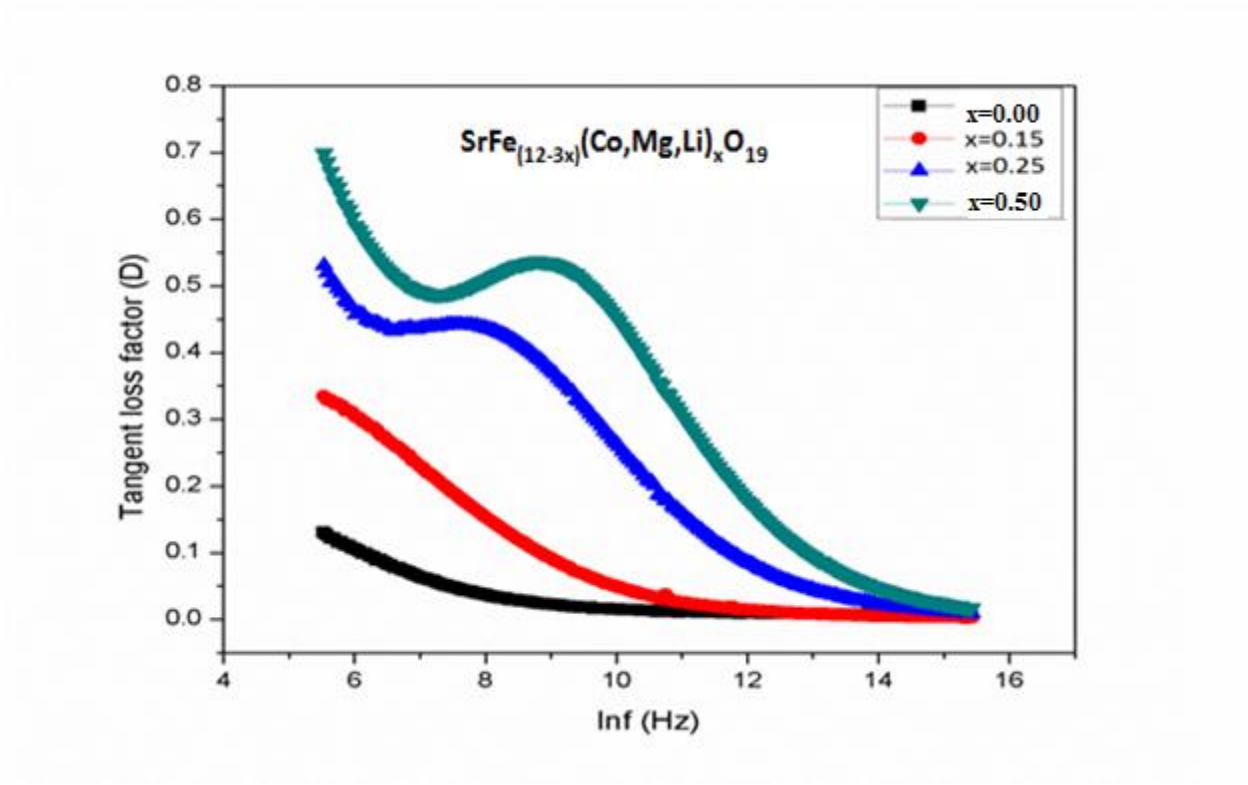

Fig 4.13 Dielectric tangent loss variation with frequency for $SrFe_{(12-3x)}(Co,Mg,Li)_xO_{19}$

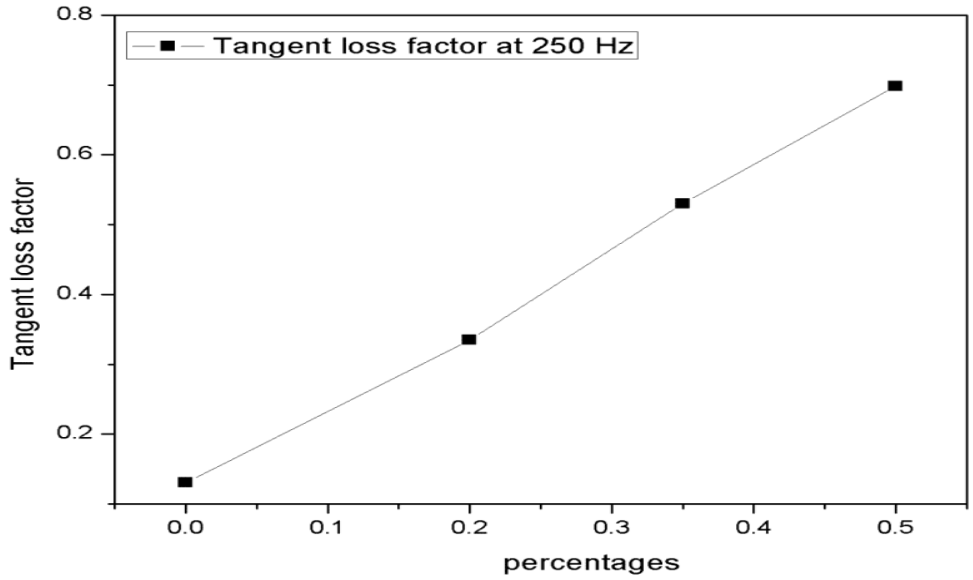

Fig 4.14 Dielectric tangent loss variation at 250 Hz for $SrFe_{(12-3x)}(Co,Mg,Li)_xO_{19}$

4.4.3 Variation of AC Conductivity

The trend of AC conductivity with frequency is given below. Following relation was used for finding our variation in Ac conductivity of Co, Mg and Li doped strontium hexaferrite nanoparticles $SrFe_{(12-3x)}(Co,Mg,Li)_xO_{19}$.

$\sigma ac = \omega \varepsilon o \varepsilon' Tan\delta$

where $\omega = 2\pi f$, εo represents the Permittivity of free space. $Tan\delta$ represents the Dissipation factor and ε' represents the Dielectric constant.

In case of Co, Mg and Li doped strontium hexaferrite the Ac conductivity shows trend which is increasing is shown in fig 4.15. by increasing the concentration of Co, Mg and Li the Ac conductivity also gets increase. The following equation shows the direct relation between dielectric loss and Ac conductivity.

$\sigma AC = \omega \varepsilon 0 \varepsilon''$

The value of Ac conductivity for pure strontium hexaferrite is $3.6*10^{-5}$ it decreases to $1.0*10^{-5}$ when concentration of Co, Mg and Li was 0.15 and it rises to $4.7*10^{-5}$ for maximum concentration of cobalt 0.50.

The values of AC conductivity for all the samples is maximum at 250 Hz frequency. The values show an increasing trend at shown in fig 4.16. For $SrFe_{(12-3x)}(Co,Mg,Li)_xO_{19}$ the value of AC conductivity is $3.10*10^{-8}$ for pure sample when x=0.00, the value increased to $1.09*10^{-7}$ when x=0.15,$3.01*10^{-7}$ when x=0.25 and $7.57*10^{-7}$ for x=0.50. The increase in Ac conductivity from $3.01*10^{-7}$ to $7.75*10^{-7}$ is seen at the same frequency of 250 Hz. The Ac conductivity varies with change in frequency.

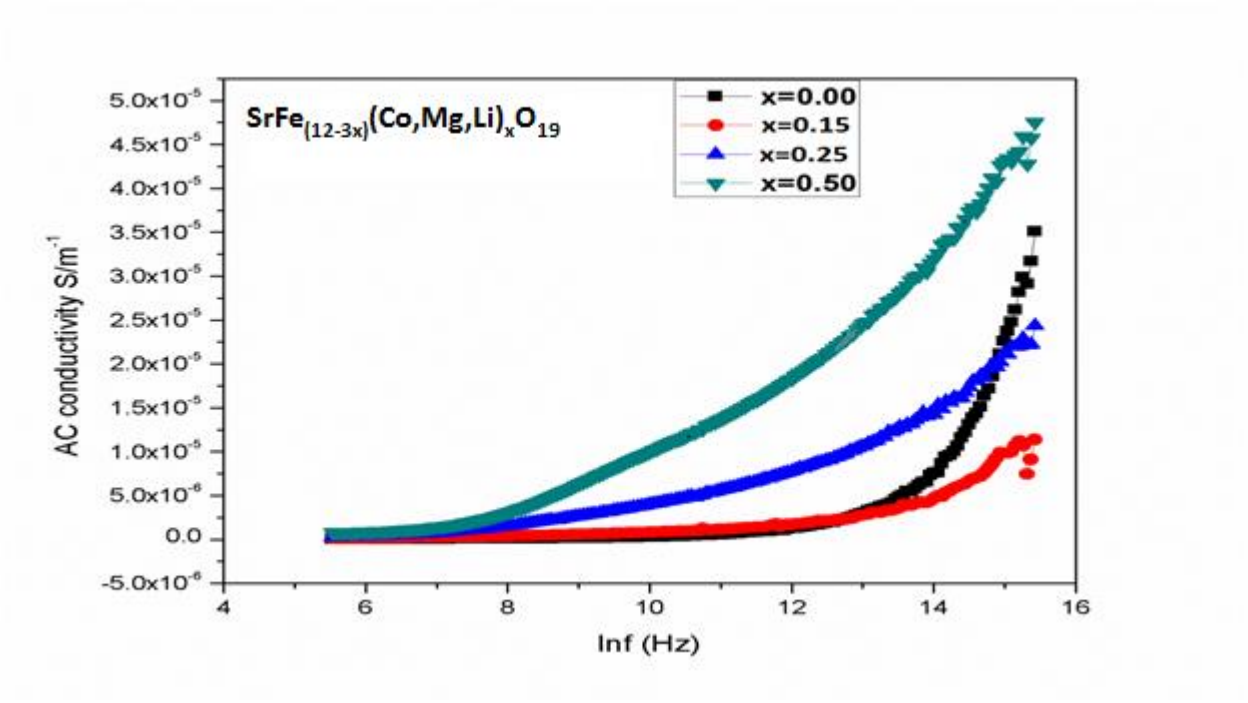

Fig 4.15 AC conductivity variation with frequency for $SrFe_{(12-3x)}(Co,Mg,Li)_xO_{19}$

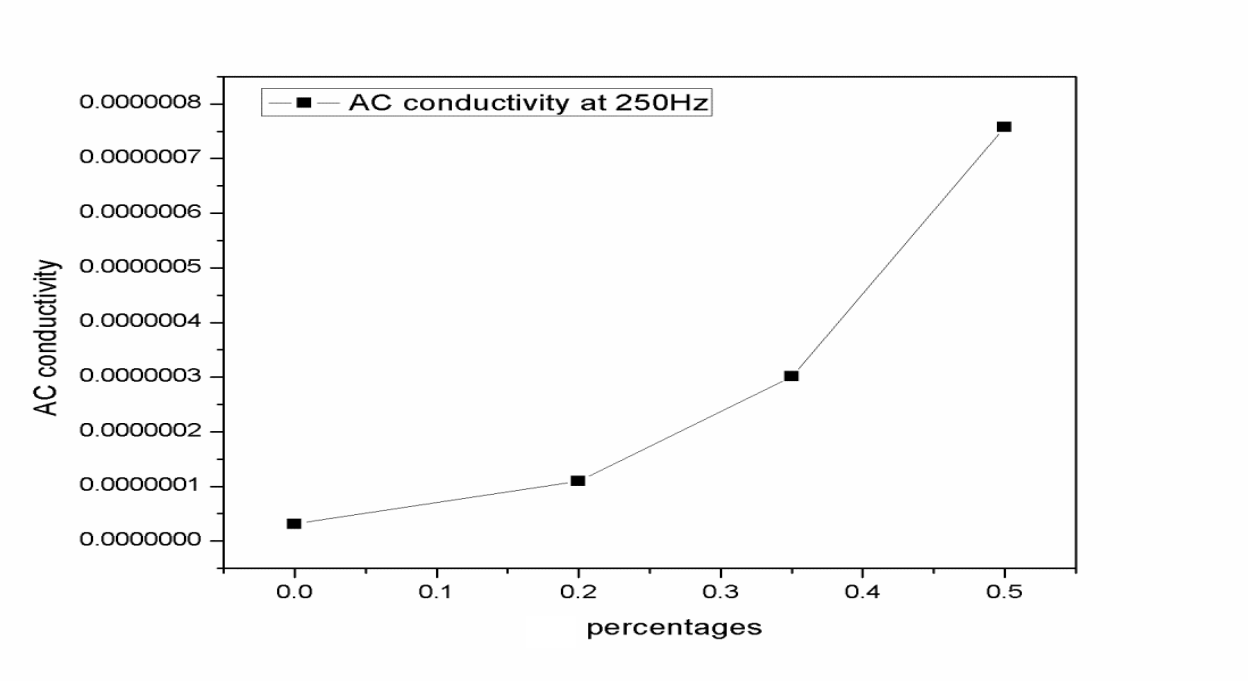

Fig 4.16 AC conductivity variation at 250 Hz for $SrFe_{(12-3x)}(Co,Mg,Li)_xO_{19}$

4.4.4 Impedance

The both imaginary part and real part components of the Conductive materials can be studied using the impedance analysis. The impedance analysis for all the prepared samples that were recorded in response to the frequency. All of these measurements were performed at room temperature. The standard equations were used for calculations.

By increasing the concentration of the Cobalt, magnesium and lithium, hopping of the charges are increased as a result the Impedance gets decrease. Due to increase in grain size there is decrease in barrier for the movement of charges, this will increase conductivity.

Real part of the impedance is shown in the figure 4.17 where a trend which is decreasing is seen. By increasing the value of x in $SrFe_{(12-3x)}(Co,Mg,Li)_xO_{19}$ the impedance gets decrease from $1.38x10^8$ to $2.33x10^7$ from x=0.00 to x=0.50, this shows conductive nature of samples increasing by addition of Co, Mg and Li.

Imaginary part of impedance is shown in fig 4.18, a decreasing trend in impedance is observed. This means by increasing the Co, Mg and Li content the impedance

decreases and the hopping of charges increases by addition of Co, Mg and Li. Increasing the percentage of Co, Mg and Li increases conductivity and decrease in resistance.

Impedance increases with decrease in frequency. Pure sample has maximum value of impedance. By adding Co, Mg and Li the conductivity of strontium hexaferrite increases by increasing Co, Mg and li concentration the barrier length decreases and charges move easily, this increase the conductivity of the material. Impedance decrease means increase in conductive nature of material.

The trend which is decreasing in value of z gives an increase in the Conductivity which will result in the decrease of the Resistance. The low values of Frequencies correspond to the higher Impedance values. This is because of the main factor of the Space Charge Polarization. It will initiate electron hopping to continue with the alternations of the applied electric field. The values of the impedance become constant at the higher Frequencies due to the reduction in the Space Charge Polarization effect.

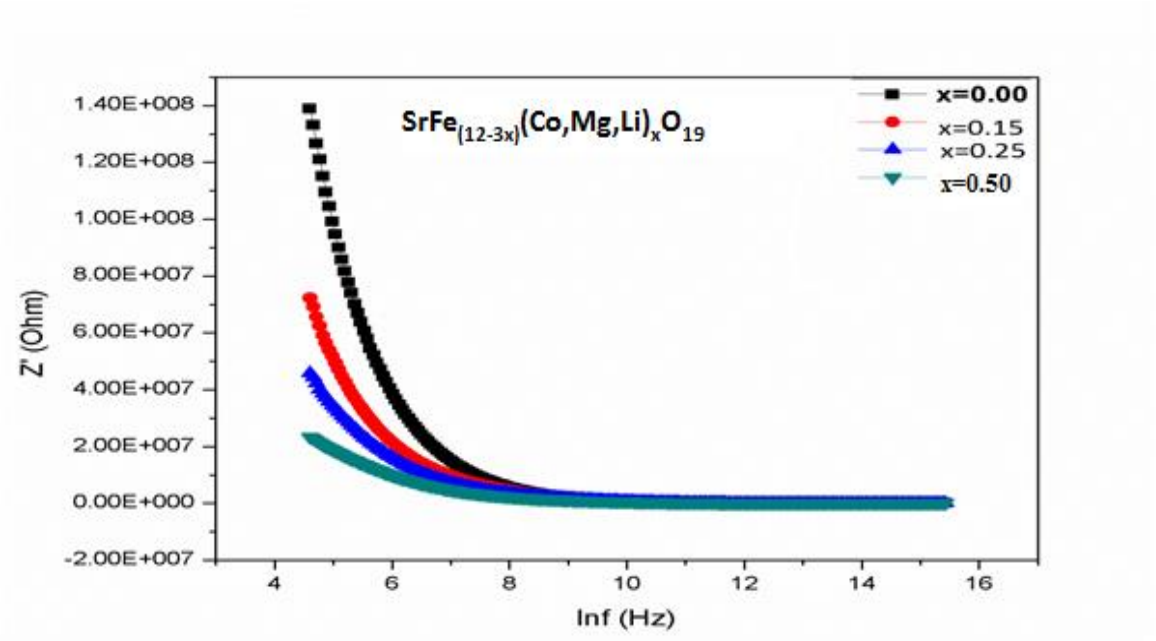

Fig 4.17 Impedance real part Z' variation with frequency for $SrFe_{(12-3x)}(Co,Mg,Li)_xO_{19}$

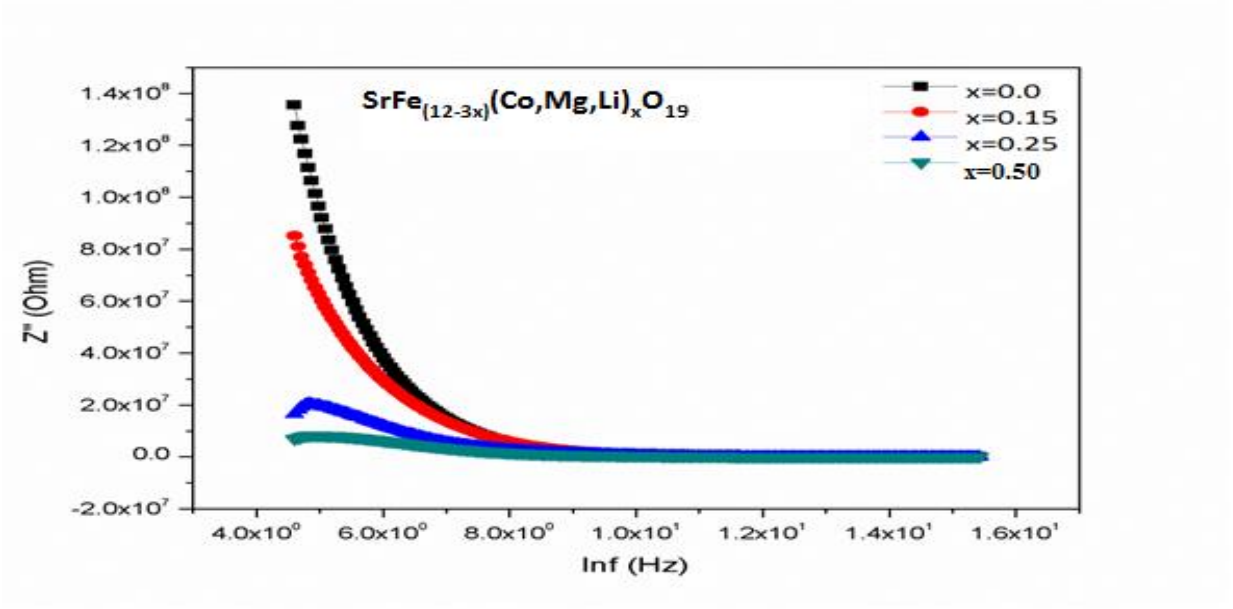

Fig 4.18 Impedance imaginary part Z" variation with frequency for $SrFe_{(12-3x)}(Co,Mg,Li)_xO_{19}$

Conclusions

In current work Co, Mg and Li dopant substitution is performed in series of $SrFe_{(12-3x)}(Co,Mg,Li)_xO_{19}$ (x=0.0,0.15,0.25,0.5) using sol gel method. The aqueous solution, containing metal nitrites were brought in use to prepare strontium hexaferrite nanoparticles. The prepared samples were calcined at 950 degrees centigrade for 3 hours. The synthesized samples were characterized with the help of X-ray diffraction (XRD), Scanning Electron microscopy(SEM), Fourier transform infra-red spectroscopy(FTIR). Impedance analyzer and LCR meter was used for performing dielectric measurements and microwave analysis.

The formation of hexagonal $SrFe_{(12-3x)}(Co,\ Mg,\ Li)_xO_{19}$ was confirmed using XRD. Debye sherrer equation was used to find out crystallite size which was in the range of 26 ±5nm. The band positions were studied using FTIR. The morphology of samples was studied through SEM.

The study of dielectric properties with change in frequency was done at room temperature. For the Co, Mg and Li $SrFe_{(12-3x)}(Co,Mg,Li)_xO_{19}$ doped strontium hexaferrite the real part of strontium hexaferrite is enhanced to 77.4 at 250 Hz for x=0.5. the values of Dielectric loss for Co, Mg and Li doped has increased from 2.2 to 54.0 at 250 Hz.

Ac conductivity values also showed increase with Co, Mg and Li doping. Ac conductivity results explains that electron hopping governs the conduction process. The impedance z for pure strontium hexaferrite is $1.40*10^8$ and is minimized to $7x10^7$ for x=0.5 in $SrFe_{(12-3x)}(Co,\ Mg,Li)_xO_{19}$. The trend which is decreasing in value of z gives an increase in the Conductivity.

The enhanced dielectric properties and increase in conductivity of the prepared nanoparticles make it applicable in field of super capacitors. the increase in conductivity makes Co, Mg and Li doped strontium hexaferrite ideal for electrical applications. The value of dielectric constant, dielectric loss, tangent loss and Ac conductivity showed their best results in sample with maximum concentration of cobalt. Hematite phase increase with doping and this can decrease the electrical

properties by further increasing the Co, Mg and Li concentration in strontium hexaferrite.

These materials are very good for use in electrical application charge storage devices and superconductors.

Future Work

The optical properties of prepared samples can be studied using UV-visible spectroscopy and can be applicable in many applications including military applications.

The composite with different polymers can be made in order to study different properties including mechanical, electrical and optical properties.

The polymerization can be used for preparing different composition of polymer blends. The effect of mechanical, dielectric and microwave properties can also be studied by making its composite with desired polymer.

The sample shows remarkable dielectric properties so they can be applicable in cathode of batteries, super capacitors or resins. These applications involve large strength and stiffness even at elevated temperatures.

The prepared samples can render very useful in various industrial applications. Properties can be varied and improve by changing percentage of ingredients.

References

[1] Ederer, C. and N.A. Spaldin, Weak ferromagnetism and magnetoelectric coupling in bismuth ferrite. Physical Review B, **71** (2005). 060401.

[2] Bedanta, S. and W. Kleemann, Supermagnetism. Journal of Physics D: Applied Physics, 42 (2008). 013001.

[3] A. N. A. Y. M. S.H. MAHMOOD1*, J. Solid State Phenomena 232 (2014) 65-92.

[4] Morin, F., Oxides which show a metal-to-insulator transition at the Neel temperature. Physical Review Letters, 3 (1959) 34.

[5] Thompson, G. and B. Evans, The structure–property relationships in M-type hexaferrites: Hyperfine interactions and bulk magnetic properties. Journal of applied physics, **73 (**1993). 6295-6297.

[6] Bilovol, V. and R. Martínez-García, Phase transformation of strontium hexagonal ferrite. Journal of Physics and Chemistry of Solids, **86 (**2015) 131-137.

[7] Hong, X., et al., A novel ternary hybrid electromagnetic wave-absorbing composite based on BaFe 11.92 (LaNd) 0.04 O 19-titanium dioxide/multiwalled carbon nanotubes/polythiophene. Composites Science and Technology, 117 (2015). 215-224.

[8] Li, J., et al., Bottom-up versus top-down effects on ciliate community composition in four eutrophic lakes (China). European journal of protistology, 53 (2016) 20-30.

[9] Gul, I., W. Ahmed, and A. Maqsood, Electrical and magnetic characterization of nanocrystalline Ni–Zn ferrite synthesis by co-precipitation route. Journal of Magnetism and Magnetic Materials,320 (2008) 270-275.

[10] Gabal, M. and Y. Al Angari, Effect of chromium ion substitution on the electromagnetic properties of nickel ferrite. Materials Chemistry and Physics,118 (2009)153-160.

[11] Valenzuela, R., Novel applications of ferrites. Physics Research International, 2012

[12] Yang, Y., et al., Efficient electrocatalytic oxygen evolution on amorphous nickel–cobalt binary oxide nanoporous layers. ACS nano, 8 (2014) 9518-9523.

[13] Zheng, F., D. Zhu, and Q. Chen, Facile Fabrication of Porous Ni x Co3–x O4 Nanosheets with Enhanced Electrochemical Performance as Anode Materials for Li-Ion Batteries. ACS applied materials & interfaces, 6 (2014). 9256-9264.

[14] Yin, Z., et al., Interface control of semiconducting metal oxide layers for efficient and stable inverted polymer solar cells with open-circuit voltages over 1.0 volt. ACS applied materials & interfaces,5 (2013) 9015-9025.

[15] Augustyn, V., P. Simon, and B. Dunn, Pseudocapacitive oxide materials for high-rate electrochemical energy storage. Energy & Environmental Science, 7 (2014) 1597-1614.

[16] Zhang, H., et al., Copper ferrite–graphene hybrid: a highly efficient magnetic catalyst for chemoselective reduction of nitroarenes. RSC Advances, 59 (2014) 31328-31332.

[17] Fu, Y., et al., Copper ferrite-graphene hybrid: a multifunctional heteroarchitecture for photocatalysis and energy storage. Industrial & Engineering Chemistry Research, 51 (2012) 11700-11709.

[18] Garcia, R.M., E.R. Ruiz, and E.E. Rams, Structural characterization of low temperature synthesized SrFe12O19. Materials Letters,50 (2001)183-187.

[19] Shirtcliffe, N.J., et al., Highly aluminium doped barium and strontium ferrite nanoparticles prepared by citrate auto-combustion synthesis. Materials research bulletin,42 (2007) 281-287.

[20] Katlakunta, S., et al., Improved magnetic properties of Cr3+ doped SrFe12O19 synthesized via microwave hydrothermal route. Materials Research Bulletin, 63 (2015) 58-66.

[21] Kaur, P., et al., Synthesis of Co-Zr doped nanocrystalline strontium hexaferrites by sol-gel auto-combustion route using sucrose as fuel and study of their structural, magnetic and electrical properties. Ceramics International,42 (2016). 14475-14489.

[22] M. S. S. Chavan, J. Magnetism and Magnetic Materials 398 (2016) 32-37.

[23] Chavan, V.C., et al., Transformation of hexagonal to mixed spinel crystal structure and magnetic properties of Co2+ substituted BaFe12O19. Journal of Magnetism and Magnetic Materials, 398 (2016) 32-37.

[24] Herme, C., P. Bercoff, and S. Jacobo, Formation of a magnetic composite by reduction of Co-Nd doped strontium hexaferrite in a hydrogen gas flow. Physica B: Condensed Matter,407 (2012) 3102-3105.

[25] Iqbal, M.J., M.N. Ashiq, and P.H. Gomez, Effect of doping of Zr–Zn binary mixtures on structural, electrical and magnetic properties of Sr-hexaferrite nanoparticles. Journal of alloys and compounds, 478 (2009). 736-740.

[26] Rashid, A.U., et al., Strontium hexaferrite (SrFe12O19) based composites for hyperthermia applications. Journal of Magnetism and Magnetic Materials, 344 (2013)134-139.

[27] Ali, A.A., et al., MWCNTs/carbon nano fibril composite papers for fuel cell and super capacitor applications. Journal of Electrostatics, 73 (2015) 12-18.

[28] Altaf, F., et al., Synthesis of Co-doped Sr-hexaferrites by Sol-gel Auto-combustion and its Electrical Characterization. Materials Today: Proceedings,2 (2015) 5548-5551.

[29] Fang, C., et al., Magnetic and electronic properties of strontium hexaferrite SrFe12O19 from first-principles calculations. Journal of Physics: Condensed Matter,15 (2003) 6229.

[30] Paladino, A., et al., Fine-Grain Nickel Ferrite for Microwave Applications at High Peak-Power Levels. Journal of Applied Physics,37 (1966) 3371-3377.

[31] E. W. D. J. S. S. M. M. L. &. L. S. Shirsath, J. Handbook of sol-gel science and technology (2018) 695-735.

[32] Al-Hartomy, O.A., et al., Dielectric and microwave properties of graphene nanoplatelets/carbon black filled natural rubber composites. International Journal of Materials and Chemistry, 2 (2012) 116-122.

[33] S. M. Waqar, J. Applied Physics 124 (2018) 286.

[34] Dang, T.M.H., et al., Sol–gel hydrothermal synthesis of strontium hexaferrite nanoparticles and the relation between their crystal structure and high coercivity properties. Advances in Natural Sciences: Nanoscience and Nanotechnology, 3 (2012) 025015.

[35] Durmus, Z., A. Durmus, and H. Kavas, Synthesis and characterization of structural and magnetic properties of graphene/hard ferrite nanocomposites as microwave-absorbing material. Journal of Materials Science, **50**(3) (2015) 1201-1213.

[36] P. S. R. J. G. Kajal K. Mallick ∗, Journal of the European Ceramic Society 27 (2007) 2045-52.

[37] Hussain, S. and A. Maqsood, Structural and electrical properties of Pb-doped Sr-hexa ferrites. Journal of Alloys and Compounds,466 (2008) 293-298.

[38] Özdemir, Z.G., et al., Super-capacitive behavior of carbon nano tube doped 11-(4-cyanobiphenyl-4-oxy) undecan-1-ol. Journal of Molecular Liquids,211 (2015) 442-447.

[39] Unakar, N.J., J.Y. Tsui, and C.V. Harding, Scanning electron microscopy. Ophthalmic Research,13 (1981). 20-35.

[40] Doyle, W.M., Principles and applications of Fourier transform infrared (FTIR) process analysis. Process Control Qual,2 (1992) 11-41.

[41] Thermo, N., Introduction to Fourier transform infrared spectrometry. Thermo Nicolet Corporation: Madison-USA, 2001.